

et al. 1998). An independent study for distal forearm BMD in Chinese (Niu et al. 1999) detected contribution of similar locus (2p23.3) expanding about 18-Mbp, which completely overlaps the formerly detected locus (about 5-Mbp; markers from D2S149 to D2S387). In the later study, several candidates, including the pro-opiomelanocortin gene (*POMC*), were proposed; however, no responsible variations have been identified as yet.

An important aspect of BMD regulation is conducted through immunological responses to inflammatory events, presumably through activation of osteoclastogenesis (Manolagas 1995; Rodan and Martin 2000). In addition to complex cytokine pathways for which the most attention have been paid, regulation through endocrine systems, notably hormonal regulation of adrenal corticoids, is important, as indicated by clinical knowledge of glucocorticoid-induced osteoporosis (Patschan et al. 2001). Moreover, higher hierarchical regulation of systemic corticoid levels, i.e., hypothalamus–pituitary–adrenal axis (HPA-axis), may have critical effects on homeostatic regulation of the immune system. Thus, genes involved in this system, such as *POMC*, should be considered for the association study.

POMC is a large precursor protein for multiple functional peptide hormones, including adrenocorticotrophic hormone (ACTH), melanocyte-stimulating hormones (alpha-MSH, beta-MSH, and gamma-MSH), and beta-endorphin. In addition to classical knowledge of influences on serum corticoid levels or on metabolic control of energy expenditure and body mass (Pritchard et al. 2002; Appleyard et al. 2003), direct and indirect effects of these peptides on the immune system have been clarified recently (Luger et al. 2003). Here, in this study, we investigated the eight single nucleotide polymorphisms (SNPs) of the *POMC* as good candidates for testing association between the genotypes and bone phenotype. In addition, to evaluate the effects on other metabolic systems, we investigated the association of body mass index (BMI) and serum cholesterol levels to the genotypes among 384 adult Japanese women.

Materials and methods

Subjects

DNA samples were obtained from peripheral blood of 384 adult Japanese women (Ishida et al. 2003; Iwasaki

et al. 2003). All were nonrelated volunteers who gave informed consent prior to the study. No participant had medical complications or was undergoing treatment for conditions known to affect bone and lipid metabolism, such as pituitary diseases, hyperthyroidism, primary hyperparathyroidism, liver disease, renal failure, adrenal diseases, or rheumatic diseases, and none was receiving estrogen replacement therapy. Physical and clinical profiles of the subjects, including age, body weight, height, BMD, plasma total cholesterol (T-chol), triglycerides, and high-density lipoprotein cholesterol (HDL-C) levels were obtained from the records of a health-check screening program. Mean values and standard deviations (SD) were 58.4 ± 8.6 (range 32–69) years for age, and 23.7 ± 3.61 kg/m² (range 14.7–38.5) for BMI. The areal BMD (expressed in grams per centimeter squared) of the distal radius, measured by dual energy X-ray absorptiometry (DXA) using DTX-200 (Osteometer Meditech Inc., Hawthorne, CA, USA) showed normal distribution (0.399 ± 0.054 g/cm²; range 0.225–0.554). Among 384 subjects, we regarded 64 individuals as low-bone-mass subjects whose adjusted BMD distributed below 0.38 (mean adjusted BMD–1SD) and 55 individuals as high-bone-mass subjects whose adjusted BMD was above 0.48 (mean adjusted BMD+1SD). Plasma lipid and lipoprotein concentrations were measured from peripheral blood collected after 12–16 h of fasting by procedures described previously (Hattori et al. 2002). All measured values were within the normal range (T-chol: 187.0 ± 32.2 mg/dl, triglycerides: 85.5 ± 59.8 mg/dl, HDL-C: 59.1 ± 12.2 mg/dl).

Genotyping for molecular variants in the *POMC* gene

Eight SNPs (Table 1) from the NCBI database (dbSNP) or the Celera database (Celera Diagnostics, Rockville, MD, USA) were selected and denoted as –2353G/A, –2345G/A, –2313A/C, –1845C/T, IVS1+267C/G, IVS2+276C/G, A132P (c.396G/C), and c.585T/C (195-Ala) according to their positions in a contig-sequence (NT_022184.13; NCBI RefSeq database) (Fig. 1a). All were confirmed to be polymorphic in our test population ($n=24$), and thus, the 384 subjects were genotyped either by cycle sequencing, TaqMan Assay (Livak 1999), or Invader assay (Mein et al. 2000) (Table 1).

For five SNPs (–2353G/A, –2313A/C, –2345G/A, –1845C/T, and A132P), cycle sequencing was carried

Table 1 Summary of polymorphisms examined at the *POMC* locus

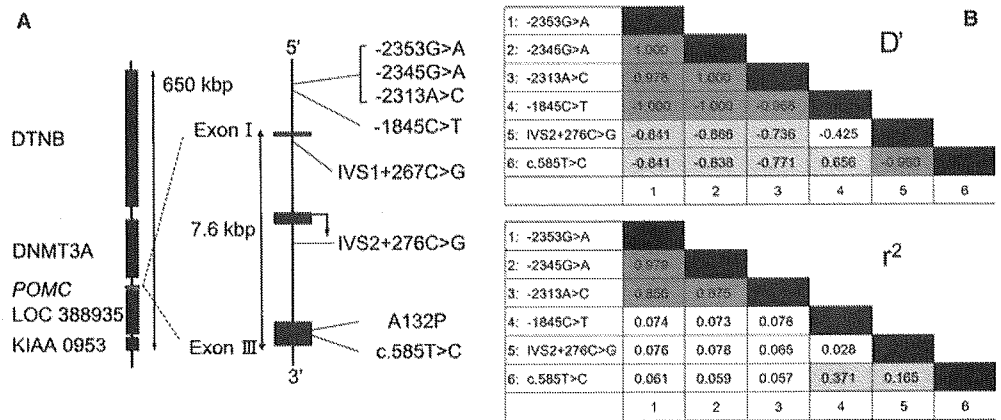
	SNP name ^a	dbSNP-ID ^b	Celera-ID ^c	Allele frequency	% heterozygosity
	–2353G/A	rs3754863		0.81:0.19	32
	–2345G/A	rs3754862		0.81:0.19	32
	–2313A/C	rs3754861		0.79:0.21	28
	–1845C/T	rs3754860		0.74:0.26	38
	IVS1+267C/G	rs1009388		0.98:0.02	5
	IVS2+276C/G	–	hCV3227244	0.68:0.32	39
	A132P	rs8192606		0.99:0.01	1
	c.585T/G	rs2071345		0.72:0.28	40

^a Location of the SNP was defined by NT_023195.12 from the NCBI RefSeq database

^b Identity number for NCBI dbSNP database

^c Identity number for Celera database

Fig. 1 Analysis of the linkage disequilibrium within the *POMC* locus. **a** Schematic diagram of the *POMC* gene showing positions of the eight examined SNPs. **b** Indices of LD, D' and r^2 were calculated on the basis of 17 estimated haplotypes (covering 100% of the chromosomes) constructed with six SNPs. Cells are highlighted with gray halftone when the D' values are greater than 0.4 or the r^2 values are greater than 0.1.



out using the BigDye terminator v1.1 Cycle Sequencing Kit (Applied Biosystems, Foster City, CA, USA) and the ABI PRISM 377 DNA Sequencing System (Applied Biosystems). The following primers were used: F-1, 5'-ACTCTTCAAGCAGATGGTGGT-3' and R-1, 5'-AGCAGGTTCTGCTGCATTA-3' (for SNP -1845C/T); F-2, 5'-AAGGCCATTGAACTGCATTAG-3' and R-2, 5'-GTCTATGTCAGACGCCTGTGGT-3' (for -2353G/A, -2313A/C and -2345G/A); and F-3, 5'-AACCCCGGAAGTACGTCAT-3' and R-3, 5'-GAAGTGCTCCATCCTGTAGGG-3' (for A132P). TaqMan assay was carried out for IVS2+4229C/G and c.585T/C, according to the manufacturers' protocol (TaqMan Assays-on-Demand; Applied Biosystems). Invader assay was carried out for IVS1+352C/G according to the manufacturers' protocol (Invader Assay: Third Wave Technologies, inc, Madison City, WI, USA) and the methods described previously (Ezura et al. 2003).

Statistical analysis

Adjusted values of BMD were obtained after normalizing the measured data with age and BMI by means of multiple regression analysis, as described previously (Iwasaki et al. 2003). Plasma lipids and lipoprotein concentrations were adjusted by reference to an age group (40–49 years) among standard data from 11,994 individuals in a 2001 cohort study for the Japanese population, using a Z-score calculation (Fujita et al. 2003).

The three genotypic categories of each SNP were converted into incremental values 0, 1, and 2, corresponding to the number of chromosomes possessing a minor allele, and quantitative association with several physical and clinical values was analyzed via one-way analysis of variance (ANOVA) with linear regression analysis as a post hoc test. The statistical significance of any correlation was accepted when the given p values of the ANOVA F test were less than 5% ($p < 0.05$). To test the existence of dominant or recessive effects of minor allele of each SNP, Student's t test was applied to compare two divided subject groups by possession of minor allele or major allele ($p < 0.05$). Distribution

analysis of contingency tables were applied for low-bone-mass ($n = 64$) or high-bone-mass individuals ($n = 55$). Chi-square test for trend was applied ($p < 0.05$). Hardy–Weinberg equilibrium among genotypes was ascertained by the chi-square test. A maximum-likelihood haplotype was estimated by the EM algorithm using Arlequin software (Genetics and Biometry Laboratory, Geneva, Switzerland) (Schneider et al. 2000), and indices of linkage disequilibrium (LD) were calculated.

Results

Eight SNPs in the *POMC* gene, one of the likely candidates for osteoporosis susceptibility, were examined in all 384 subjects. Allelic frequencies and genotypic frequencies were clarified and showed no deviation from Hardy–Weinberg equilibrium (Table 1). By excluding the data from two rare SNPs (IVS1+352C/G and A132P), we estimated haplotype frequencies from available genotypic data for the other six SNPs. The LD analysis, evaluated by D' and r^2 for every combination of SNPs, indicated apparent LD within the locus (Fig. 1b). Especially strong LD was detected among -2353G/A, -2345G/A, and -2313A/C ($D' > 0.97$, $r^2 > 0.85$).

By examining a correlation between SNP genotype and adjusted BMD for each of the eight SNPs (Table 2), significant correlation was evident with three promoter SNPs (-2353G/A, -2345G/A, and -2313A/C). For the most significant -2353G/A ($r = -0.16$, $p = 0.0020$), codominant BMD lowering effect of the minor A-allele was indicated where homozygous carriers of G-alleles had the highest values (0.405 ± 0.054 g/cm²), heterozygous individuals were intermediate (0.390 ± 0.053 g/cm²), and homozygous A-allele carriers had the lowest adjusted BMDs (0.369 ± 0.048 g/cm²) (Fig. 2a). Dominant or codominant effect was supported by analyzing the differences between two genotypically divided groups based on dominant model (A-allele carriers: $n = 132$, adj-BMD = 0.388 ± 0.053 ; and noncarriers: $n = 242$, adj-BMD = 0.405 ± 0.054 , $p = 0.004$, Student's t test) and recessive model (G-allele carriers: $n = 365$, adj-BMD = 0.400 ± 0.054 ; and noncarriers: $n = 9$,

Table 2 Summary of the regression analysis of *POMC* variations among 384 subjects. *BMD* bone mineral density

SNP name	Number ^a	Major homo (<i>n</i>)	Hetero (<i>n</i>)	Minor homo (<i>n</i>)	Correlation coefficient	<i>p</i> value
Adjusted BMD (g/cm ²)						
-2353G/A	374	0.405 ± 0.054 (242)	0.390 ± 0.053 (123)	0.369 ± 0.048 (9)	-0.16	0.002
-2345G/A	374	0.404 ± 0.055 (244)	0.391 ± 0.052 (121)	0.369 ± 0.048 (9)	-0.14	0.005
-2313A/C	374	0.404 ± 0.055 (244)	0.392 ± 0.052 (106)	0.376 ± 0.051 (24)	-0.15	0.004
-1845C/T	375	0.397 ± 0.052 (206)	0.402 ± 0.057 (143)	0.403 ± 0.055 (26)	0.05	0.35
IVS1 + 267C/G	329	0.401 ± 0.056 (314)	0.376 ± 0.050 (15)	(-)	0.09	0.09
IVS2 + 276C/G	376	0.401 ± 0.057 (184)	0.398 ± 0.051 (145)	0.401 ± 0.056 (47)	-0.02	0.76
A132P	373	0.399 ± 0.055 (367)	0.425 ± 0.038 (4)	(-)	0.05	0.35
c.585T/G	377	0.397 ± 0.054 (195)	0.401 ± 0.054 (151)	0.409 ± 0.063 (31)	0.06	0.28
Adjusted total cholesterol (mg/dl)						
-2353G/A	374	189.4 ± 34.0 (242)	183.2 ± 27.9 (123)	174.9 ± 16.7 (9)	-0.11	0.036
-2345G/A	374	189.6 ± 34.0 (244)	182.7 ± 27.8 (121)	174.9 ± 16.7 (9)	-0.12	0.024
-2313A/C	374	189.6 ± 34.0 (244)	183.4 ± 27.1 (106)	176.7 ± 27.3 (24)	-0.12	0.019
-1845C/T	375	186.9 ± 32.1 (206)	186.2 ± 29.8 (143)	195.1 ± 42.7 (26)	0.04	0.479
IVS1 + 267C/G	329	187.3 ± 32.0 (314)	185.7 ± 27.1 (15)	(-)	-0.01	0.848
IVS2 + 276C/G	376	185.0 ± 29.7 (184)	185.1 ± 32.9 (145)	195.8 ± 32.2 (47)	0.08	0.100
A132P	373	186.8 ± 32.2 (367)	192.3 ± 58.1 (4)	(-)	0.02	0.737
c.585T/G	377	186.0 ± 30.2 (195)	187.3 ± 33.4 (151)	187.8 ± 35.3 (31)	0.02	0.683

^a represents the number of genotyped subjects

^b *p* values are calculated for the regression analysis with ANOVA *F* test

adj-BMD = 0.369 ± 0.048, *p* = 0.09, Student's *t* test). The other two promoter SNPs also demonstrated allelic-dosage effects (data not shown). By comparing the distribution of genotypically divided subjects among low-bone-mass individuals (*n* = 64; 36, 25, and three individuals for G/G, A/G, and A/A genotypes, respectively) and high-bone-mass individuals (*n* = 55; 43 and 12 individuals for G/G and A/G; no individual for A/A), significant difference with trend was detected (*p* = 0.006), indicating minor A-allele of -2353G/A could be a genetic risk for low-bone-mass trait.

We examined whether these variations correlated with other clinical features (Table 2). The same three promoter SNPs (-2353G/A, -2345G/A, and -2313A/C) demonstrated significant correlation to adjusted T-chol levels (ex; -2313A/C; *r* = -0.12, *p* = 0.019) (Fig. 2b). No significant correlations were detected

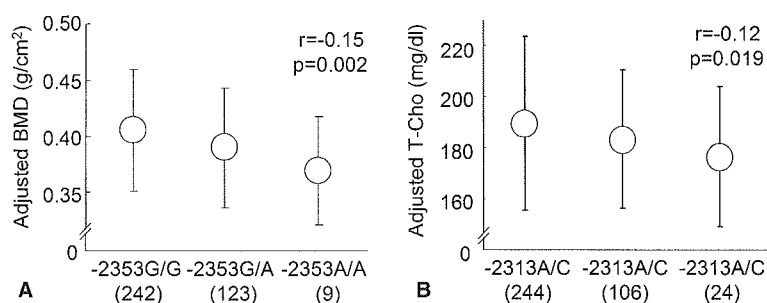
between other covariates (age, body weight, height, BMI or adjusted plasma HDL-C and triglyceride levels) and any SNPs.

Discussion

In the work reported here, we detected significant association between genotypes of three *POMC* variations (-2353G/A, -2345G/A, and -2313A/C) and adjusted levels of radial BMD among adult Japanese women. In addition, the same promoter SNPs showed an association with plasma T-chol level but not with body mass. These data indicated possible influences of *POMC* polymorphism(s) on bone-mineral status for the first time, as well as on lipoprotein metabolism.

Association of promoter SNP genotype to low-bone-mass phenotype indicates that the altered level of *POMC* peptide might affect the bone metabolism. Lowered BMD can result from accelerated bone loss and/or deficient acquisition of bone mass (Riggs and Melton 1986). However, because bone loss caused by systemic corticoid use is thought to occur mainly through resorption (Weinstein et al. 2002, 2004), *POMC* variations would also affect resorptive mechanisms. In addition, anabolic aspect of corticoid function should be

Fig. 2 Effects of *POMC* variations on adjusted bone mineral density (BMD) and total cholesterol (T-chol) in plasma. Adjusted BMD levels were plotted against three genotypically classified subgroups at the -2353G/A SNP site. Adjusted T-chol levels were plotted against genotypically classified subgroups at -2313A/C site. The allelic-dosage effects of these variants on BMD or T-chol were analyzed by linear regression as a post-hoc test of ANOVA. Calculations of *p* values were based on *F* tests. *Open circles* indicate mean values, *error bars* indicate standard deviations



considered on the skeletal system through multiple pathways (Patschan et al. 2001). In the feedback system of HPA-axis, multiple cross-talks between the corticotropin releasing hormone, somatostatin growth hormone system, gonadotropin system, and thyroid hormone are known. Longitudinal studies in large cohorts, as well as functional studies, may clarify the molecular events by which SNPs in the *POMC* promoter bring about alterations in bone metabolism. Presumably, these variation(s) affect transcription of the ACTH-precursor peptide, which should affect secretion of ACTH from the anterior pituitary and/or the regulation of other *POMC*-derived peptide hormones. The consequent effects on bone metabolism might, in turn, introduce variation in BMD in an adult woman. Those assumptions should be validated by additional studies.

As mentioned, *POMC* was selected as a candidate because it is a precursor of ACTH. Although its function on the skeletal system may mainly depend on the catabolic aspect of corticoids, alternative pathways would also contribute, as described. In addition, other *POMC*-derived peptides, such as MSHs, could be responsible for alterations in bone metabolism. Anti-inflammatory function of alpha-MSH through effects on macrophages has been reported (Star et al. 1995). Also, alpha-MSH and beta-endorphin functioning in body-mass maintenance and in energy expenditure may contribute to bone-mass regulation because a close relationship between these two regulatory systems has been assumed (Reid 2002).

Interrelationship between these clinical phenotypes has been documented: Individuals carrying *POMC* mutations that impair synthesis of ACTH and alpha-MSH were reported to become obese (Krude et al. 1998). In addition, linkage and association of the *POMC* locus were reported for the serum leptin level (Hixson et al. 1999), fasting insulin level (Santoro et al. 2004), and obesity (Delplanque et al. 2000). However, in our test subjects, we detected no significant correlation between the SNP genotype and the indices of obesity; thus, the correlation we observed between BMD and the SNP genotypes was not secondary to altered body mass. Instead, we found an association between variant -2313A/C and adjusted T-chol. Although the detected correlation was weak and reproducibility of this finding or the correlation between the low-density lipoprotein cholesterol (LDL-C) and the genotype was not investigated in our study, the possibility has to be examined in a future study as to whether *POMC*-derived peptides regulate lipoprotein metabolism through a distinctive mechanism.

Another of our findings, the existence of strong LD among the three significantly BMD-correlated promoter SNPs, may imply an important promoter/enhancer function of the region they share up-stream of the *POMC* coding sequence. In fact, a computer algorithm, MatInspector program v2.2 (Quandt et al. 1995), predicted that two of these three SNPs were part of presumed consensus binding sequences of known tran-

scription factors; i.e., -2345G/A in the acute myeloid leukemia (AML) -1a binding sequence (TGCGGT; underlined "G" is a variant nucleotide) and -2353G/A in the GATA-1 or GATA-2 sequence (CGAGATCGCG; underlined "G" is a variant nucleotide). The functional significance of these *cis* elements and *trans* factors remains to be clarified. Of course, our study does not stipulate specific SNP(s) that functionally regulate BMD. Thus, we cannot rule out the possibility that these polymorphic markers at chromosome 2 (2p23) may themselves be in linkage disequilibrium with other, unmeasured functional variants (see Fig. 1). Functional studies as well as longitudinal studies will be required to find a true mechanistic basis for the associations reported here.

In summary, we have shown a significant association of three variations in the promoter region of the *POMC* gene (-2353G/A, -2345G/A, and -2313A/C) with radial BMD levels among adult Japanese women. An association was also detected between these SNPs and plasma cholesterol levels. Structural inspection proposed that transcription factors AML-1a and GATA-1 or -2 might bind to sequences containing these SNP sites. Detailed investigations involving molecules of the HPA axis may clarify the true mechanism of BMD regulation by *POMC* SNPs.

Acknowledgements We thank Mina Kodaira, Miho Kawagoe, and Naoko Tsuruta for their expert technical assistance. This work was supported by a grant for Strategic Research from the Ministry of Education, Science, Sports and Culture of Japan; by a Research Grant for Research from the Ministry of Health and Welfare of Japan; and by a Research for the Future Program Grant of The Japan Society for the Promotion of Science.

References

- Albagha OM, Ralston SH (2003) Genetic determinants of susceptibility to osteoporosis. *Endocrinol Metab Clin North Am* 32:65-81
- Appleyard SM, Hayward M, Young JI, Butler AA, Cone RD, Rubinstein M, Low MJ (2003) A role for the endogenous opioid beta-endorphin in energy homeostasis. *Endocrinology* 144:1753-1760
- Delplanque J, Barat-Houari M, Dina C, Gallina P, Clement K, Guy-Grand B, Vasseur F, Boutin P, Froguel P (2000) Linkage and association studies between the proopiomelanocortin (*POMC*) gene and obesity in caucasian families. *Diabetologia* 43:1554-1557
- Devote M, Shimoya K, Caminis J, Ott J, Tenenhouse A, Whyte MP, Sereda L, Hall S, Considine E, Williams CJ, Tromp G, Kuivaniemi H, Ala-Kokko L, Proskop DJ, Spotila LD (1998) First-stage autosomal genome screen in extended pedigrees suggests genes predisposing to low bone mineral density on chromosomes 1p, 2p and 4p. *Eur J Hum Genet* 6:151-157
- Ezura Y, Kajita M, Ishida R, Yoshida S, Yoshida H, Suzuki T, Hosoi T, Inoue S, Shiraki M, Orimo H, Emi M (2003) Association of multiple nucleotide variations in the pituitary glutamyl cyclase gene (*QPCT*) with low radial BMD in adult women. *J Bone Miner Res* 19:1296-1301
- Fujita Y, Ezura Y, Emi M, Sato K, Takada D, Iino Y, Katayama Y, Takahashi K, Kamimura K, Bujo H, Saito Y (2003) Hypercholesterolemia associated with splice-junction variation of inter-alpha-trypsin inhibitor heavy chain 4 (*ITIH4*) gene. *J Hum Genet* 49:24-28

- Hattori H, Hirayama T, Nobe Y, Nagano M, Kujiraoka T, Egashira T, Ishii J, Thuji M, Emi M (2002) Eight novel mutations and functional impairments of the LDL receptor. *J Hum Genet* 47:80–87
- Hixson JE, Almasy L, Cole S, Birnbaum S, Mitchell BD, Mahaney MC, Stern MP, MacCluer JW, Blangero J, Comuzzie AG (1999) Normal variation in leptin levels is associated with polymorphisms in the proopiomelanocortin gene, POMC. *J Clin Endocrinol Metab* 84:3187–3191
- Ishida R, Ezura Y, Emi M, Kajita M, Yoshida H, Suzuki T, Hosoi T, Inoue S, Shiraki M, Ito H, Orimo H (2003) Association of a promoter haplotype (–1542G/–525C) in the tumor necrosis factor receptor associated factor-interacting protein gene with low bone mineral density in Japanese women. *Bone* 33:237–241
- Iwasaki H, Emi M, Ezura Y, Ishida R, Suzuki T, Hosoi T, Inoue S, Shiraki M, Swensen J, Orimo H (2003) Association of a Trp16Ser variation in the gonadotropin releasing hormone signal peptide with bone mineral density, revealed by SNP-dependent PCR typing. *Bone* 32:185–190
- Kanis JA, Melton LJ, Christiansen C, Johnston CC, Khaltayev N (1994) The diagnosis of osteoporosis. *J Bone Miner Res* 9:1137–1141
- Krude H, Biebermann H, Luck W, Horn R, Brabant G, Gruters A (1998) Severe early-onset obesity, adrenal insufficiency and red hair pigmentation caused by POMC mutations in humans. *Nat Genet* 19:155–157
- Liu YZ, Liu YJ, Robert RR, Deng HW (2003) Molecular studies of identification of genes for osteoporosis: the 2002 update. *Endocrinology* 177:147–196
- Livak KJ (1999) Allelic discrimination using fluorogenic probes and the 5' nuclease assay. *Genet Anal* 14:143–149
- Luger TA, Scholzen TE, Brzoska T, Bohm M (2003) New insights into the functions of alpha-MSH and related peptides in the immune system. *Ann NY Acad Sci* 994:133–140
- Manolagas SC (1995) Role of cytokines in bone resorption. *Bone* 17:63–67
- Mein CA, Barratt BJ, Dunn MG, Siegmund T, Smith AN, Esposito L, Nutland S, Stevens HE, Wilson AJ, Phillips MS, Jarvis N, Law S, de Arruda M, Todd JA (2000) Evaluation of single nucleotide polymorphism typing with invader on PCR amplicons and its automation. *Genome Res* 10:330–343
- Niu T, Chen C, Cordell H, Yang J, Wang B, Wang Z, Fang Z, Nicholas JS, Clifford JR, Xu X (1999) A genome-wide scan for loci linked to forearm bone mineral density. *Hum Genet* 104:226–233
- Patschan D, Loddenkemper K, Buttgerit F (2001) Molecular mechanisms of glucocorticoid-induced osteoporosis. *Bone* 29:498–505
- Peacock M, Turner CH, Econs MJ, Foroud T (2002) Genetics of osteoporosis. *Endocrinol Rev* 23:303–326
- Pritchard LE, Turnbull AV, White A (2002) Pro-opiomelanocortin processing in the hypothalamus: impact on melanocortin signaling and obesity. *J Endocrinol* 172:411–421
- Quandt K, Frech K, Karas H, Wingender E, Werner T (1995) MatInd and MatInspector: new fast and versatile tools for detection of consensus matches in nucleotide sequence data. *Nucleic Acids Res* 23:4878–4884
- Reid IR (2002) Relationships among body mass, its components, and bone. *Bone* 31:547–555
- Riggs BL, Melton LJ III (1986) Involutional osteoporosis. *N Engl J Med* 314:1676–1686
- Rodan GA, Martin TJ (2000) Therapeutic approaches to bone diseases. *Science* 289:1508–1514
- Santoro N, del Giudice EM, Cirillo G, Raimondo P, Corsi I, Amato A, Grandone A, Perrone L (2004) An insertional polymorphism of the proopiomelanocortin gene is associated with fasting insulin levels in childhood obesity. *J Clin Endocrinol Metab* 89:4846–4849
- Schneider S, Roessli D, Excoffier L (2000) Arlequin ver. 2.000: a software for population genetics data analysis. Genetics and Biometry Laboratory, University of Geneva, Geneva, Switzerland
- Star RA, Rajora N, Huang J, Stock RC, Catania A, Lipton JM (1995) Evidence of autocrine modulation of macrophage nitric oxide synthase by alpha-melanocyte-stimulating hormone. *Proc Natl Acad Sci USA* 92:8016–8020
- Weinstein RS, Chen JR, Powers CC (2002) Inhibition of osteoblastogenesis and promotion of apoptosis of osteoblasts and osteocytes by glucocorticoids. *J Clin Invest* 109:1041–1048
- Weinstein RS, Jia D, Powers CC, Stewart SA, Jilka RL, Parfitt AM, Manolagas SC (2004) The skeletal effects of glucocorticoid excess override those of orchidectomy in mice. *Endocrinology* 145:1980–1987

Expression of estrogen-responsive finger protein (Efp) is associated with advanced disease in human epithelial ovarian cancer

Michiko Sakuma^{a,*}, Jun-ichi Akahira^{a,b}, Takashi Suzuki^b, Satoshi Inoue^c, Kiyoshi Ito^a,
Takuya Moriya^b, Hironobu Sasano^b, Kunihiro Okamura^a, Nobuo Yaegashi^a

^aDepartment of Obstetrics and Gynecology, Tohoku University Graduate School of Medicine, 1-1 Seiryō-machi, Aoba-ku, Sendai 980-8574, Japan

^bDepartment of Pathology, Tohoku University Graduate School of Medicine, Sendai, Japan

^cDivision of Gene Regulation and Signal Transduction, Research Center for Genomic Medicine, Saitama Medical School, Saitama, Japan

Received 28 March 2005

Available online 2 September 2005

Abstract

Objective. The estrogen-responsive ring finger protein (Efp) gene, one of estrogen receptor (ER) target genes, is considered to be essential for estrogen-dependent cell proliferation. To understand the estrogenic action on ovarian cancer, we studied the relationships between Efp and ERs expressions and the correlations of Efp expression with clinicopathological parameters in epithelial ovarian cancer.

Methods. The protein expressions for Efp, ER α and ER β were examined by immunoblotting in 12 ovarian cancer cell lines. Efp mRNA expressions were evaluated by quantitative RT-PCR in 12 ovarian cancer cell lines. A total of 100 surgical specimens diagnosed as epithelial ovarian cancer were examined immunohistochemically using antibodies for Efp, ER α and ER β .

Results. Efp protein was detected in 8 out of 12 cell lines. In Efp protein-positive cell lines, Efp mRNA was expressed higher than that in negative ($P = 0.021$). All of the Efp protein-positive cell lines simultaneously expressed either ER α or ER β protein. By immunohistochemical staining, Efp immunoreactivity was detected in 63 out of 100 ovarian cancer specimens and positive signals were in the cytoplasm of carcinoma cells. There were significant correlations between Efp and ER α , ER β immunoreactivity (Efp and ER α , $P = 0.022$; Efp and ER β , $P = 0.032$). Efp expression was significantly higher in a subgroup with serous adenocarcinoma ($P = 0.010$) and with advanced disease ($P = 0.026$). No significant relationship was detected between Efp immunoreactivity and overall survival.

Conclusion. The expression of Efp was detected in human epithelial ovarian cancer and high expression of Efp was correlated with advanced disease and serous adenocarcinoma, and ERs status.

© 2005 Elsevier Inc. All rights reserved.

Keywords: Efp; Ovarian cancer; Immunohistochemistry; Estrogen receptor

Introduction

Estrogen and progesterone are sex steroid hormones that are secreted from the ovary and cause the development of the female sex organs. They are also recognized as a significant modifier of the growth, development, invasion and metastasis of gynecological cancers. The actions of estrogen are mediated through specific ligand receptors. There are two receptor subtypes for estrogen, estrogen receptor- α

(ER α) and estrogen receptor- β (ER β) [1,2]. It is assumed that these receptors, members of the steroid/thyroid hormone receptor superfamily mediate these actions by binding ligand dependently to the estrogen-responsive element (ERE) that is located in the promoter region of target genes, thus directly regulating their transcription [3,4]. A variety of estrogenic functions are characterized by the expression of the estrogen-responsive genes following the binding of receptor protein to EREs [5,6].

Estrogen-responsive finger protein (Efp) is a member of the Ring-finger B-box Coiled-Coil family that is thought to be involved in the regulation of various cellular functions, including cell-cycle regulation and gene transcription [5,7].

* Corresponding author. Fax: +81 22 717 7258.

E-mail address: msakuma@mail.tains.tohoku.ac.jp (M. Sakuma).

Efp has been isolated from human genomic DNA binding-site cloning using a recombinant ER protein [5]. Efp gene has an estrogen-responsive element (ERE) in an exon corresponding with the 3'-untranslated region of mRNA [5,8]. Efp is widely expressed in various organs and structures such as the genital tracts, thyroid gland, aorta, spleen, kidney and brain [9]. Estrogen-induced Efp expression is found in the uterus, brain and mammary gland cells [5,8], and its expression is co-localized with ER [9]. A study of knock-out mice has revealed that Efp is essential for cell growth mediated by estrogen in the uterus [6], suggesting that Efp is essential for estrogen mediated cell growth.

Efp expression in the context of cancer has been studied predominantly in breast cancer. Efp mRNA was detected in the MCF-7 human breast carcinoma cell line, where it was induced by estrogen treatment within 0.5 h [10], suggesting that Efp can mediate estrogen actions such as cell growth as a primary responsive gene in breast cancer [10,11]. Recently, it has been suggested that negative cell-cycle regulators, such as 14-3-3 sigma are reduced in Efp-positive breast cancer cells because Efp targets 14-3-3 sigma for proteolysis as an ubiquitin ligase [11]. Thus, Efp may play roles not only as an estrogen target gene but also as a cell-cycle regulator.

Epithelial ovarian cancer is the leading cause of death due to a gynecological malignancy in the great majority of developed countries [12,13]. Sex steroid hormones have been implicated in the etiology and/or progression of some epithelial ovarian cancers, but the possible biological significance of steroid hormone actions in these cancers remains controversial [14–17]. The expression of Efp has not been examined in human epithelial ovarian cancer tissues, and thus the biological significance of Efp expression and correlation between the expression of Efp and ERs expression in this cancer have not yet been studied. We need to understand the new molecular targets or biological makers related to estrogenic actions for ovarian cancer as well as for those associated with breast cancer. In the current study, we examined the expression of Efp in human ovarian cancer tissues and cell lines.

Materials and methods

Cell lines

We used 12 ovarian carcinoma cell lines, two normal ovarian surface epithelial cell lines and one breast cancer cell line as follows. The seven cell lines OVCAR3, Caov3, SKOV3, TOV112D, TOV21G, OV90 and ES2 (adenocarcinoma OVCAR3, SKOV3; serous adenocarcinoma Caov3, OV90; clear cell adenocarcinoma TOV21G, ES2; endometrioid adenocarcinoma TOV112D) were purchased from American Type Culture Collection. The five cell lines JHOS2, JHOS3, HTOA, OMC3 and JHOC5 (serous adenocarcinoma JHOS2, JHOS3, HTOA; mucinous adenocarci-

noma OMC3; clear cell adenocarcinoma JHOC5) were purchased from Riken cell bank (Tsukuba, Japan). Two cell lines OSE2 and OSE4 established from normal ovarian epithelial cells were kindly provided by the Department of Obstetrics and Gynecology, Kumamoto University School of Medicine, Kumamoto, Japan [18]. MCF-7 (the human breast cancer cell line) was provided by the Institute of Department, Aging and Cancer, Tohoku University, Sendai, Japan. Cell lines were maintained in DMEM/F12 medium (Invitrogen, CA, USA), supplemented with 10% fetal bovine serum and 1% penicillin/streptomycin (Invitrogen) and incubated in a 5% CO₂ atmosphere at 37°C.

Surgical specimens and clinical data

We examined surgical specimens from a total of 100 cases of common epithelial ovarian carcinoma obtained from patients treated between 1988 and 2000 at Tohoku University Hospital, Sendai, Japan. Information regarding age, performance status on admission, histology, stage, grade, residual tumor after primary surgery and overall survival was retrieved from the review of patient charts. Median follow-up time for patients was 59 months (range, 4–120 months). Of the 100 patients, 77 (77%) received optimal cytoreduction at time of surgery, 84 (84%) patients received platinum-based chemotherapy postoperatively. Patients with stage Ia disease, low grade-disease (G1, G2) or poor performance status did not receive platinum-based chemotherapy. Performance status was defined according to WHO criteria (World Health Organization, 1979). Histology, stage and grade were according to FIGO criteria (International Federation of Gynecology and Obstetrics; [19]). Residual tumor was determined by the amount of unresectable tumor left following primary cytoreductive surgery. Optimal cytoreduction was defined as no gross residual tumor or less than 2 cm in diameter, whereas suboptimal cytoreduction was defined as any gross residual tumor remaining 2 cm or residual tumor greater than 2 cm in diameter. Overall survival was calculated from the time of initial surgery to death or the date of the last contact. Survival times of patients still alive or lost to follow-up were censored as of December 2002. All of these archival specimens were retrieved from the surgical pathology files at Tohoku University Hospital, Sendai, Japan. The informed consent was obtained from each patient. These specimens were all fixed in 10% formalin and embedded in paraffin. The research protocol was approved by the Ethics Committee of Tohoku University Graduate School of Medicine, Sendai, Japan.

Quantitative reverse transcription-PCR

Total RNA was isolated from cells by phenol-chloroform extraction using Isogen (Nippon gene, Tokyo, Japan). RNA was treated with RNase-free DNase (Roche Diagnostics; 1 µg/µl) for 2 h at 37°C, followed by heat inactivation at 65°C for 10 min. A reverse transcription (RT)-PCR kit (SUPER-

SCRIPT II First-strand synthesis system, Invitrogen) was used and cDNA synthesis was carried out according to the manufacturer's instructions. cDNAs were synthesized from 5 µg of total RNA using random hexamer and RT was carried out for 50 min at 42°C with SUPERSCRIPT II reverse transcriptase. Quantitative PCR was performed using an iCycler system (Bio-Rad, Tokyo, Japan). For the determination of Efp cDNA content, a 25 µl-reaction mixture consisting of 23 µl iQ™ SYBR Green MasterMix, 1 µl each primer and 1 µl of template cDNA was prepared. PCR conditions were as follows: 2-min denaturation at 90°C, 30-s annealing at 60°C (for Efp), 62°C (for β-actin) and 1.5-min extension at 72°C. Primers for PCR reactions were as follows: Efp-F, 5'-CGTGGAGTGGTTCAACAC-3' and Efp-R, 5'-GAGCAGATGGAGATGGTG-3' (1689–1923, 234 base pairs, bp); β-actin-F, 5'-CCAACCGCGAG-AAGATGAC-3' and β-actin-R, 5'-GGAAGGAAGGCTG-GAAGAGT-3' (382–841, 459 bp). In initial experiments, following amplification, PCR products were purified and subjected to direct sequencing to verify amplification of correct sequences (ABI prism 310 Genetic Analyzer, Applied Biosystems, CA, USA). β-Actin primers were utilized as a positive control and Efp expression level was calculated as value of Efp RT-PCR divided by value of β-actin RT-PCR. Negative controls without RNA and without reverse transcriptase were also performed.

Immunoblotting

Cells were grown to 70% confluence in 10-cm plates and after removal of culture medium with Phosphate-buffered saline (PBS). Whole-cell protein concentration was measured by Model 680 microplate reader (Biorad, USA) using Bradford reagent (Biorad). A rabbit polyclonal antibody against Efp protein was made by one of the authors (SI). Mouse monoclonal antibody for ERα was purchased from NOVOCASTRA (Newcastle, UK). Mouse monoclonal antibody for ERβ was purchased from GeneTex, Inc. (TX, USA). In all, 20 µg of protein of each sample was mixed with an equal volume of 2× concentrated sodium dodecyl sulfate (SDS)-polyacrylamide gel electrophoresis (SDS-PAGE) sample buffer, boiled and then electrophoresed on 7% ready-made gels containing SDS (Mini Protein II Western blotting system, Biorad). Proteins were then transferred to nitrocellulose membrane (Hybond PDVF, Biorad). The membranes were incubated in blocking solution (PBS containing 5% nonfat milk and 0.05% Tween-20), then incubated in 1:4000 dilution of Efp antibody (1:100 for ERα, 1:1500 for ERβ and 1:1000 for β-actin) in blocking solution overnight at 4°C. After incubation with horseradish peroxidase (HRP)-labeled anti-rabbit IgG (anti-mouse IgM for ERα and ERβ) (Vector Laboratories, USA), the antigen–antibody complex was visualized with ECL system (Amersham, Germany). The MCF-7 breast cancer cell line was used as positive control. Actin (Ab-1, Oncogene) was used as an internal positive control.

Immunohistochemistry and scoring of immunostaining

Immunohistochemical analysis was performed using a streptavidin–biotin amplification method using the Histofine Kit (Nichirei, Tokyo, Japan). For antigen retrieval, slides were heated in an autoclave at 120°C for 5 min in citric acid buffer (2 mM citric acid and 9 mM trisodium citrate hydrate, pH 6.0). The dilutions of primary antibodies for Efp, ERα and ERβ were 1:2000, 1:50 and 1:1500, respectively. The antigen–antibody complex was visualized with 3,3'-diaminobenzidine (DAB) solution (1mM DAB, 50mM Tris–HCl buffer (pH 7.6) and 0.006% H₂O₂), and counterstained with hematoxylin. The ER positive normal breast tissue was used as a positive control. For statistical analysis of Efp immunoreactivity, we classified carcinomas into two groups: +, positive carcinoma cells; and –, no immunoreactivity. For evaluation of ERα and ERβ immunoreactivity, we used the H score system to count carcinoma cells as described previously [20,21]. Scores were generated as follows: (3 × [percentage of strongly staining cells]) + (2 × [percentage of moderately staining cells]) + (1 × [percentage of weakly staining cells]). This scoring system yielded results ranging from 0 to 300. Evaluation was carried out independently by two of the authors (MS and JA) for at least 500 cells.

Statistical analysis

Statistical analysis was performed using Stat View 5.0 (SAS Institute Inc., NC, USA) software. The correlation between expression of Efp mRNA and protein was also assessed using the Mann–Whitney *U* test. The statistical significance between Efp immunoreactivity and clinicopathological parameters was evaluated using Friedman's χ^2 -test. The correlation between Efp and ERα, ERβ immunoreactivity was assessed using the Mann–Whitney *U* test. The univariate analysis of prognostic significance was performed using the log-rank test after each survival curve was obtained by the Kaplan–Meier method. All patients who could be assessed were included in the intention-to-treat analysis. A result was considered significant when the *P* value was less than 0.05.

Results

First, we examined Efp expression in ovarian cancer cells. By immunoblotting with anti-Efp antibody, immunoreactive bands corresponding to Efp, sized at approximately 70 kDa, were detected in 8 out of 12 ovarian cancer cell lines (Fig. 1). Efp expression in cell lines was supported with data obtained by quantitative RT-PCR study. Of the 12 ovarian cancer cell lines, 8 were positive for Efp protein expression by immunoblotting showing relatively higher levels of Efp-mRNA than seen in the 4 cell lines negative for Efp protein expression (Fig. 2) (*P* = 0.021). From these

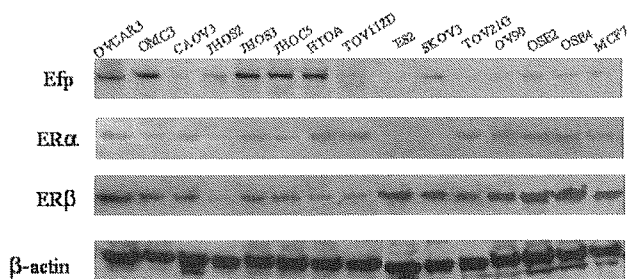


Fig. 1. Immunoblotting with variable cell lines, the top panel with anti-Efp antibody, the second panel with anti-ER α antibody, the third panel with anti-ER β antibody and the bottom panel with anti- β -actin antibody. OVCAR3, OMC3, CAO3, JHOS2, JHOS3, JHOC5, HTOA, TOV112D, ES2, SKOV3, TOV21G and OV90 were derived from ovarian cancer. OSE2 and OSE4 were derived from normal ovarian surface epithelium. MCF-7 was a cell line derived from breast cancer and used as a positive control of Efp and ERs expressions. β -Actin was used as an internal positive control of antibody.

results, we were convinced that cell lines established from not only normal ovarian epithelium but also ovarian cancers expressed Efp genes at various levels similar to results seen with breast cancer cell lines.

Because the Efp gene was expressed by estrones through estrogen receptors, we next examined ERs protein expression in these cell lines (Fig. 2). By immunoblotting with anti-ER α antibody, 10 out of 12 ovarian cancer lines and the 2 cell lines from normal ovarian epithelium showed positive bands. All cell lines positive for Efp protein expression, except SKOV3, were simultaneously positive to ER α . Similarly, all cell lines showed positive bands for ER β by immunoblotting with anti-ER β antibody. From these results, we knew that all of the Efp-immunoreactive cell lines simultaneously expressed either ER α or ER β protein.

Then, we performed immunohistochemical staining with anti-human Efp antibody for the 100 surgical specimens diagnosed as ovarian cancer to confirm Efp expression in ovarian cancer tissues. Efp protein expression was detected in 63 out of 100 specimens (63%). Positive staining was observed in the cytoplasm of ovarian cancer cells (Figs. 3A, D).

We then compared Efp expression and various clinicopathological parameters; results are summarized in Table 1. Differences by histological types were detected in Efp expression, i.e., the subgroup of serous adenocarcinomas showed significantly higher incidence of Efp positivity than other subgroups ($P = 0.010$). Similarly, the subgroup of advanced-stage disease showed a significantly higher incidence of Efp positivity than the subgroup consisting of early-stage disease ($P = 0.026$). There were no significant relationships between Efp immunoreactivity and patient age, performance status, histological grade or residual tumor (Table 1).

We decided to examine simultaneous ER and Efp expression in cancer tissues because Efp is mainly transactivated by ERs. Immunohistochemical studies showed that all ovarian cancer tissues were positive for both ER α and ER β to a greater or lesser extent, and immunopositive

signals were confined exclusively to the nuclei of tumor cells (Figs. 3B, C, E, F). The median H scores for ER α in Efp-immunopositive and Efp-immunonegative tumors were 80.1 ± 70.3 and 39.5 ± 59.4 (mean \pm SD), respectively, indicating that Efp-positive cancers expressed significantly higher levels of ER α than Efp-negative cancers ($P = 0.022$). In the same way, the median H score for ER β in Efp-immunopositive and Efp-immunonegative tumors was 67.7 ± 56.2 and 43.0 ± 43.7 (mean \pm SD), respectively, indicating that Efp-positive cancers expressed significantly higher levels of ER β than Efp-negative cancers ($P = 0.032$). Interestingly, the subgroup of serous adenocarcinomas showed significantly higher H scores (112.1 ± 60.7) than those of the other subgroups (29.7 ± 51.8) ($P < 0.0001$). In contrast, this tendency was not observed in immunoreactivity of ER β among each histologic subgroup (data not shown).

Finally, we examined the possibility of Efp as a clinical prognostic factor by univariate analysis. As shown in Table 2, clinical variables including histologic type, grade, stage and residual tumor size were all significantly related with overall survival. These results seem to be consistent with data described previously [13,22,23]. With regard to analysis of Efp expression, we did not find any significant correlation between Efp immunoreactivity and overall survival ($P = 0.78$).

Discussion

In this study, we found strong correlations between Efp and ER α and between Efp and ER β in ovarian cancer tissues; we also found that both ER α and ER β proteins were expressed in most cancer cell lines with positive for Efp protein. Efp mRNA and protein are up-regulated by

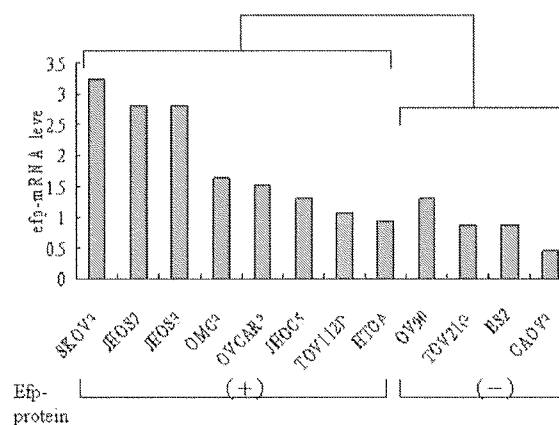


Fig. 2. Quantitative RT-PCR for expression of Efp mRNA in ovarian cancer cell lines. RT-PCR reactions were performed for each samples, and the ratio of Efp/ β -actin was calculated and normalized. The left 8 cell lines were positive for Efp protein by immunoblotting, as determined from results of Fig. 1. Efp mRNA expression among cell lines positive for Efp protein was significantly higher than those among cell lines that are negative.

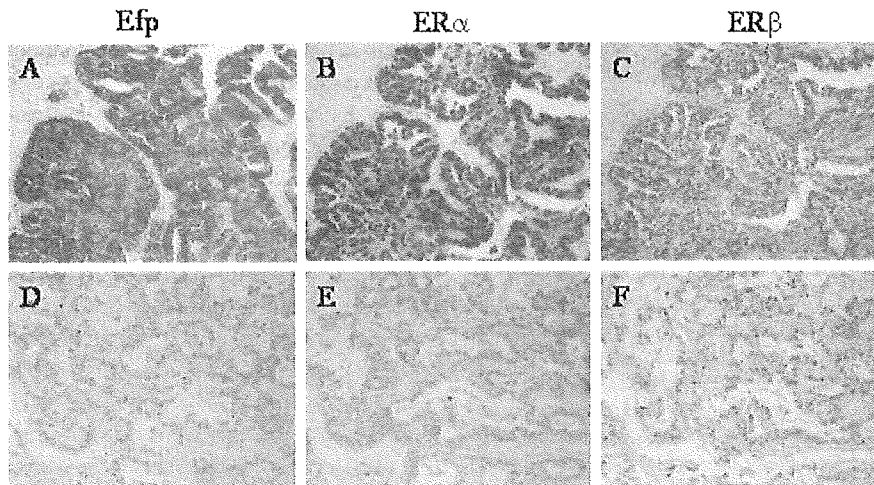


Fig. 3. Immunohistochemistry for Efp, ER α and ER β in ovarian cancer tissues. Serial sections of each surgical specimens were stained with anti-Efp (A and D), anti-ER α (B and E) and anti-ER β (C and F) antibodies, respectively. Representative data positive for each antibody (A–C) and negative (D–F) were shown. Positive signals for Efp were detected on the cytoplasm of cancer cells and positive signals for both ER α and ER β were confined to the nuclei of cancer cells.

estrogen treatment in vivo [5,8]. Estrogen-responsive proliferation of uterine cells which express abundant ER α was impaired in Efp knock-out mice, suggesting that Efp is a mediator of cell proliferation as one of the direct targets of ER α [6]. In breast cancer, which is considered one of the

sex steroid hormone-related malignant neoplasms, the Efp promoter could be enhanced by both ER α and ER β in the setting of estrogen treatment. It has been suggested that Efp responds to estrogen as a common downstream gene of ER α and ER β and that Efp mediates estrogen action in both ER α - and ER β -positive breast cancer [10]. Results from our present study are consistent with these previous reports focusing on breast cancer [6,10], and suggest that Efp may mediate estrogen action through ER α and ER β in some human epithelial ovarian cancer tissues and cell lines.

However, responsiveness and prognosis impact of steroid hormone in ovarian cancer may be different from those in breast cancer. Responsiveness to hormonal manipulation clearly results in favorable feature of breast cancer. It is known that most of the ER-positive breast cancers are primarily responsive to endocrine therapy, but breast cancer lacking any ER expression often reveals more aggressive phenotypes and is resistant to endocrine therapy [24]. Human epithelial ovarian cancer is believed to be a sex steroid hormone-related neoplasm, although the biological significance and the prognostic impact of hormone receptors are still controversial [14–17]. Previous studies have suggested a relation between progesterone receptor expression and favorable prognosis of epithelial ovarian cancer; especially, tumors of ER-negative/PR-positive showed a significantly superior prognosis when compared with the other combinations [14,25,26]. These evidences suggest that

Table 1
Association between Efp immunoreactivity and clinicopathological parameters in human epithelial ovarian cancer

	Total	Efp immunoreactivity		P value
		+	–	
		63	37	
Age				
≤ 50	50	33	17	NS
> 50	50	30	20	
Performance status				
0, 1	70	44	26	NS
2, 3, 4	30	19	11	
Histological type				
Serous	43	34	9	0.01
Mucinous	14	10	4	
Endometrioid	15	7	8	
Clear cell	27	11	16	
Squamous cell	1	1	0	
Histological grade				
Grade 1	41	23	18	NS
Grade 2	35	22	13	
Grade 3	24	18	6	
Stage				
I, II	55	23	22	0.026
III, IV	45	40	15	
Residual tumor				
≤ 2 cm	59	34	25	NS
> 2 cm	41	29	12	
ER α H score		80.1 \pm 70.3	39.6 \pm 59.4	0.022
ER β H score		67.7 \pm 56.2	43.0 \pm 43.7	0.032

Histological type: serous, serous adenocarcinoma; mucinous, mucinous adenocarcinoma; endometrioid, endometrioid adenocarcinoma; clear cell, clear cell adenocarcinoma; squamous, squamous cell carcinoma.

Table 2
Univariate analysis of overall survival

Variable	P value
Efp immunoreactivity (+ vs. –)	0.78
Histological type	0.018
Histological grade	0.0085
Stage	< 0.0001
Residual tumor	< 0.0001

estrogen function in ovarian cancer has some differences from that in breast cancer, and this may be a reason why Efp expression was unrelated to survival in this study.

Efp immunoreactivity was associated in the current study with the histologic type, serous adenocarcinoma. Ovarian cancer is a morphologically, histologically and biologically heterogeneous disease, which has likely contributed to difficulties in defining the molecular alterations associated with development and progression. On the basis of morphological and histologic criteria, there are four major types of primary ovarian carcinomas: serous adenocarcinoma, mucinous adenocarcinoma, endometrioid adenocarcinoma and clear cell adenocarcinoma. Some molecular studies have offered support for the hypothesis that different histologic types of ovarian carcinoma likely represent distinct disease entities. For example, serous adenocarcinomas demonstrate frequent *p53* mutations and more than 85% of mucinous ovarian adenocarcinomas show *K-ras* mutations [27,28]. Endometrioid adenocarcinomas preferentially exhibit microsatellite instability and mutations of *CTNGB1* (β -catenin) [29,30]. Considering estrogenic action on ovarian cancer, which still remains controversial, it has been thought that ERs expression and its transcriptional gene expression differ in each histologic type. A higher expression of ER α relative to expression of ER β has been observed in surface epithelial ovarian cancer compared with normal ovarian surface epithelium [2,31]. As for histologic type, there is a relative paucity of ER α expression in clear cell adenocarcinoma compared with the level of expression in serous, endometrioid and mucinous adenocarcinoma [32]. In epithelial ovarian cancer, especially in serous adenocarcinoma, the germ line mutations of BRCA1 have been observed as frequently as seen in breast cancer. The BRCA1 gene has been found to inhibit signaling by ligand-activated ER α through the estrogen-responsive enhancer element and to block the transcriptional activation domain of ER α , AF-2 [33,34]. Our results, together with those of previous reports, suggest that the expression of Efp might be one of the different characteristics of each histologic type and that Efp overexpression especially correlates with serous histology, as the result of estrogen actions through ERs.

Early stages of ovarian cancer are generally asymptomatic and difficult to detect, thus, by the time clinical diagnosis made, most of patients have widespread tumor dissemination beyond the ovaries. Despite a high response rate to first-line chemotherapy, the prognosis of these women is poor, with the 5-year overall survival only 10–20% [13,22]. We need some markers of ovarian cancer to identify subpopulations of patients whose disease is progressive and behaves differently from those in the majority of patients, and which might therefore benefit from adapted therapeutic options. To our knowledge, this current report is the first to evaluated the relationships between Efp and clinicopathological parameters in epithelial ovarian cancer. In our study, the expression of Efp had no prognostic value but was related to advanced-stage disease.

Our results suggest that overexpression of Efp might cause invasive and progressive characteristics of epithelial ovarian cancer, if so Efp might have the potential to be useful as a biological marker.

The benefit of optimal surgery for patients with advanced ovarian cancer is well established [35]. Recently, Levine et al. reported that genetic differences failed to predict for outcome of surgical cytoreduction [36]. Our result that the expression of Efp did not correlate with residual tumor size after primary cytoreductive surgery is consistent with this previous report. With regard to tumor dissemination in the abdominal cavity, intrapelvic location of ovaries and their mobility in relation to adjacent structures might be in more relation to ability of optimal surgery than the genetic changes. These evidences suggest that some genetic differences including Efp expression could clarify a character of tumors but would not predict clinical outcome in epithelial ovarian cancer.

From our experimental data, the expression of Efp was detected in human epithelial ovarian cancer and correlated with ERs status, advanced-stage disease and serous adenocarcinoma histologic type. It has been suggested that the expression of Efp in human epithelial ovarian cancer relates to regulation of cell proliferation and carcinogenesis through ERs and that Efp could be a biological marker of this cancer. Further investigations are required to reveal the roles of Efp related to estrogenic action and cell-cycle regulation in epithelial ovarian cancer.

Acknowledgments

This work was supported in part by a grant-in-aid for Scientific Research from the Ministry of Health and Welfare, a grant-in-aid from the Ministry of Education, Science and Culture, a grant-in-aid from Kurokawa Cancer Research Foundation, a grant-in-aid from Japan Gynecologic Oncology Group (JGOG) and the 21st Century Center of Excellence (COE) Program Special Research Grant from the Ministry of Education Science, Sports and Culture.

References

- [1] Enmark E, Gustafsson JA. Oestrogen receptors—An overview. *J Int Med* 1999;246:133–8.
- [2] Li AJ, Baldwin RL, Karlan BY. Estrogen and progesterone receptor subtype expression in normal and malignant ovarian epithelial cell cultures. *Am J Obstet Gynecol* 2003;189:22–7.
- [3] Evans RM. The steroid and thyroid hormone receptor family. *Science* 1988;240:889–95.
- [4] Green S, Chambon P. Nuclear receptors enhance our understanding of transcription regulation. *Trends Genet* 1988;11:309–14.
- [5] Inoue S, Orimo A, Hosoi T, et al. Genomic binding-site cloning reveals an estrogen-responsive gene that encodes a RING finger protein. *Proc Natl Acad Sci U S A* 1993;99:11117–21.
- [6] Orimo A, Inoue S, Minowa O, et al. Underdeveloped uterus and reduced estrogen responsiveness in mice with disruption of the

- estrogen responsive finger protein gene, which is a direct target of estrogen receptor α . *Proc Natl Acad Sci U S A* 1999;96:12027–32.
- [7] Ikeda K, Inoue S, Orimo A, et al. Multiple regulatory elements and binding protein of the 5'-flanking region of the human estrogen-responsive finger protein (efp) gene. *Biochem Biophys Res Commun* 1997;236(3):765–71.
- [8] Orimo A, Inoue S, Ikeda K, Noji S, Muramatsu M. Molecular cloning, structure, and expression of mouse estrogen-responsive finger protein Efp. *J Biol Chem* 1995;270(41):24406–13.
- [9] Shimada N, Suzuki T, Inoue S, et al. Systemic distribution of estrogen-responsive finger protein (Efp) in human tissues. *Mol Cell Endocr* 2004;218:147–53.
- [10] Ikeda K, Orimo A, Higashi Y, Muramatsu M, Inoue S. Efp as a primary estrogen-responsive gene in human breast cancer. *FEBS* 2000;472:9–13.
- [11] Horie K, Urano T, Ikeda K, Inoue S. Estrogen-responsive RING finger protein controls breast cancer growth. *J Steroid Biochem Mol Biol* 2003;85:101–4.
- [12] Akahira JI, Aoki M, Suzuki T, et al. Expression of EBAG9/RCAS1 is associated with advanced disease in human epithelial ovarian cancer. *Br J Cancer* 2004;90:2197–202.
- [13] Akahira JI, Yoshikawa H, Shimizu Y, et al. Prognostic factors of stage IV epithelial ovarian cancer: a multicenter retrospective study. *Gynecol Oncol* 2001;81:398–403.
- [14] Akahira J, Inoue T, Suzuki T, et al. Progesterone receptor isoforms A and B in human epithelial ovarian carcinoma: immunohistochemical and RT-PCR studies. *Br J Cancer* 2000;83(11):1488–94.
- [15] Bizzi A, Codegoni AM, Landoni F, et al. Steroid receptors in epithelial ovarian carcinoma: relation to clinical parameters and survival. *Cancer Res* 1988;48:6222–6.
- [16] Masood S, Heitmann J, Nuss RC, Benrubi GI. Clinical correlation of hormone receptor status in epithelial ovarian cancer. *Gynecol Oncol* 1989;34:57–60.
- [17] Rao BR, Slotman BJ. Endocrine factors in common epithelial ovarian cancer. *Endocr Rev* 1991;12:14–26.
- [18] Nitta M, Katabuchi H, Ohtake H, et al. Characterization and tumorigenicity of human ovarian surface epithelial cells immortalized by SV40 large T antigen. *Gynecol Oncol* 2001;81:10–7.
- [19] Shimizu Y, Kamoi S, Amada S, et al. Toward the development of a universal grading system for ovarian epithelial carcinoma: I. Prognostic significance of histopathologic features-problems involved in the architectural grading system. *Gynecol Oncol* 1998;70:2–12.
- [20] Akahira J, Suzuki T, Ito K, et al. Differential expression of progesterone receptor isoforms A and B in the normal ovary, and in benign, borderline, and malignant ovarian tumors. *Jpn J Cancer Res* 2002;93:807–15.
- [21] McCarty KS Jr, Miller LS, Cox EB, Konrath J, McCarty KS Sr. Estrogen receptor analysis. *Arch Pathol Lab Med* 1985;109:716–21.
- [22] Bonnefoi H, A'Hern RP, Fisher C, et al. Natural history of stage IV epithelial ovarian cancer. *J Clin Oncol* 1999;17(3):767–75.
- [23] Munkarah AK, Hallum III AV, Morris M, et al. Prognostic significance of residual disease in patients with stage IV epithelial ovarian cancer. *Gynecol Oncol* 1997;64(1):13–7.
- [24] Clarke R, Skaar T, Baumann K, et al. Hormonal carcinogenesis in breast cancer: cellular and molecular studies of malignant progression. *Breast Cancer Res Treat* 1994;31:237–48.
- [25] Lindgren P, Backstrom T, Mahlek CG, et al. Steroid receptors and hormones in relation to cell proliferation and apoptosis in poorly differentiated epithelial ovarian tumors. *Int J Oncol* 2001;19(1):31–8.
- [26] Munstedt K, Steen J, Knauf AG, et al. Steroid hormone receptors and long term survival in invasive ovarian cancer. *Cancer* 2000;89(8):1783–91.
- [27] Anttila M, Kosma VM, Ji H, et al. Clinical significance of alpha-catenin, collagen IV, and Ki-67 expression in epithelial ovarian cancer. *J Clin Oncol* 1998;16(8):2591–600.
- [28] van der Zee AG, Hollema H, Suurmeijer AJ, et al. Value of P-glycoprotein, glutathione *S*-transferase pi, c-erbB-2, and p53 as prognostic factors in ovarian carcinomas. *J Clin Oncol* 1995;13(1):70–8.
- [29] Aunoble B, Sanches R, Didier E, Bignon YJ. Major oncogenes and tumor suppressor genes involved in epithelial ovarian cancer [review]. *Int J Oncol* 2000;16:567–76.
- [30] Feeley KM, Wells M. Precursor lesions of ovarian epithelial malignancy. *Histopathology* 2001;38:87–95.
- [31] Pujol P, Rey JM, Nirde P, et al. Differential expression of estrogen receptor- α and β messenger RNAs as a potential maker of ovarian carcinogenesis. *Cancer Res* 1998;58:5367–73.
- [32] Fujimura M, Hidaka T, Kataoka K, et al. Absence of estrogen receptor- α expression in human ovarian clear cell adenocarcinoma compared with ovarian serous, endometrioid, and mucinous adenocarcinoma. *Am J Surg Pathol* 2001;25(5):667–72.
- [33] Aida H, Takakuwa K, Nagata H, et al. Clinical futures of ovarian cancer in Japanese woman with germ-line mutations of BRCA1. *Clin Cancer Res* 1998;4(1):235–40.
- [34] Fan S, Wang JA, Yuan R, et al. BRCA1 inhibition of estrogen receptor signaling in transfected cells. *Science* 1999;284:1354–6.
- [35] Chi DS, Franklin CC, Levine DA, et al. Improved optimal cytoreduction rares for stage IIIc and IV epithelial ovarian, fallopian tube, and primary peritoneal cancer: a change in surgical approach. *Gynecol Oncol* 2004;94:650–4.
- [36] Levine D.A., Bonome T., Olshen A.B., et al. Gene expression profiling of advanced ovarian cancers to predict the outcome of primary surgical cytoreduction. *ASCO* 2004:448 [abstr 5000].

Survival Versus Apoptotic 17 β -Estradiol Effect: Role of ER α and ER β Activated Non-genomic Signaling

FILIPPO ACCONCIA,¹ PIERANGELA TOTTA,¹ SUMITO OGAWA,² IRENE CARDILLO,¹ SATOSHI INOUE,² STEFANO LEONE,¹ ANNA TRENTALANCE,¹ MASAMI MURAMATSU,² AND MARIA MARINO^{1*}

¹Department of Biology, University "Roma Tre," Rome, Italy

²Research Center for Genomic Medicine, Saitama Medical School, Saitama, Japan

The capability of 17 β -estradiol (E2) to induce the non-genomic activities of its receptors (ER α and ER β) and to evoke different signaling pathways committed to the regulation of cell proliferation has been analyzed in different cell cancer lines containing transfected (HeLa) or endogenous (HepG2, DLD1) ER α or ER β . In these cell lines, E2 induced different effects on cell growth/apoptosis in dependence of ER isoforms present. The E2–ER α complex rapidly activated multiple signal transduction pathways (i.e., ERK/MAPK, PI3K/AKT) committed to both cell cycle progression and apoptotic cascade prevention. On the other hand, the E2–ER β complex induced the rapid and persistent phosphorylation of p38/MAPK which, in turn, was involved in caspase-3 activation and cleavage of poly(ADP-ribose)polymerase, driving cells into the apoptotic cycle. In addition, the E2–ER β complex did not activate any of the E2–ER α -activated signal molecules involved in cell growth. Taken together, these results demonstrate the ability of ER β isoform to activate specific signal transduction pathways starting from plasma membrane that may justify the effect of E2 in inducing cell proliferation or apoptosis in cancer cells. In particular this hormone promotes cell survival through ER α non-genomic signaling and cell death through ER β non-genomic signaling. *J. Cell. Physiol.* 203: 193–201, 2005.

© 2004 Wiley-Liss, Inc.

Knowledge of the molecular mechanism by which estrogens exert pleiotropic functions in different tissues and organs has evolved rapidly during the past two decades. In particular, the mechanism by which 17 β -estradiol (E2) induces cell proliferation has been the object of extensive studies in several tissues (Sutherland et al., 1983; Marino et al., 1998, 2001; Castoria et al., 1999, 2001; Razandi et al., 1999). However, recent reports demonstrated that E2 could even decrease cell growth by significantly increasing apoptosis in breast cancer MCF-7 cell variants, prostate cells, and several other cell types (see Song and Santen, 2003 for review). Whether the E2 apoptotic effects can be explained by the expression of different estrogen receptor (ER) isoforms (i.e., ER α and ER β) is presently unknown.

It has been assumed that E2 exerts survival proliferative effects mainly by rapid non-genomic mechanisms originating from the hormone binding to ER α (Marino et al., 1998, 2002; Castoria et al., 1999, 2001; Lobenhofer et al., 2000; Fernando and Wimalasena, 2004). In line with this assumption, E2 treatment of MCF-7 cells triggers association of ER α with Src kinase and p85, the regulatory subunit of PI3K, leading to DNA synthesis (Castoria et al., 2001). Moreover, E2 induces rapid non-genomic pathways and DNA synthesis even in ER α transiently transfected cell lines (e.g., Chinese hamster ovary, CHO; cervix epitheloid carcinoma cell line, HeLa) (Razandi et al., 1999; Marino et al., 2002). In addition, multiple and parallel signal transduction pathways are rapidly activated by the E2–ER α complex in hepatoma, HepG2, cells (e.g., ERK/MAPK, PI3K/AKT) (Marino et al., 2003). The disruption of such membrane starting pathways completely prevents the E2-induced DNA synthesis and the cyclin D₁ expression at the specific response elements, activator protein-1 (AP-1) and stimulating protein-1 (SP-1) (Marino et al., 2002, 2003). All these results point to the concept that ER α is the primary endogenous mediator of rapid E2 actions committed to cell proliferation.

Less information is available on the role played by ER β in E2 proliferative effects. Data from cell cultures, gene expression, and knockout mice clearly indicate that E2-activated ER β may function as a tumor suppressor by modulating the proliferative effects of ER α (Couse and Korach, 1999; Weihua et al., 2003; Cheng et al., 2004; Paruthiyil et al., 2004; Strom et al., 2004). These studies support a functional antagonism between ER α and ER β with respect to the E2-induced cell proliferation, but do not clarify either the putative role of ER β in E2-induced apoptosis or the signal transduction pathways involved. However, the ability of E2–ER β complex to activate rapid non-genomic mechanisms has been reported. A subpopulation of ER β transfected into CHO cells is membrane bound and capable of activating IP₃ production, ERK/MAPK and c-Jun kinase phosphorylation (Razandi et al., 1999). Recently, Gerales and coworkers (Gerales et al., 2003) reported that E2 reduces ERK/MAPK activity through ER β stimulation in porcine smooth muscle cells. Moreover, conflicting

Abbreviations: E2, 17 β -estradiol; E2-BSA, β -estradiol 6-(*o*-carboxy-methyl)oxime:BSA; ER, estrogen receptor; ERE, estrogen responsive element; ERK, extracellular regulated kinase; MAPK, mitogen-activated protein kinase; PI3K, phosphoinositide-3-kinase; PKC, protein kinase C; PARP, poly(ADP-ribose) polymerase.

Contract grant sponsor: MURST; Contract grant sponsor: University "Roma Tre"; Contract grant number: RBAU01TXN3_001; Contract grant sponsor: FIRB 2001 and 2004 University "Roma Tre".

*Correspondence to: Maria Marino, Department of Biology, University "Roma Tre," Viale G. Marconi, 446, I-00146 Rome, Italy. E-mail: m.marino@uniroma3.it

Received 4 June 2004; Accepted 29 July 2004

DOI: 10.1002/jcp.20219

evidences on the ability of ER β to activate or inactivate Src and p38 kinases (Castoria et al., 2001; Kousteni et al., 2001; Geraldles et al., 2003; Mori-Abe et al., 2003) has been also reported. In particular, the existence of non-genomic mechanism(s) underlying the antiproliferative effects of E2-ER β complex is to date completely unknown.

Here, the ability of E2 to induce ERs activities has been studied in the HeLa cells devoid of any ERs and rendered E2-sensitive by transient transfection with human ER α or ER β expression vectors. We report that E2 induced different effects on cell growth/apoptosis decision in the presence of the two different isoforms of receptor. The E2-ER α complex activated multiple signal transduction pathways (i.e., ERK/MAPK, PI3K/AKT, p38/MAPK) involved in cell cycle progression, whereas the E2-ER β complex activated only p38/MAPK, which in turn, drives cells to apoptosis. A role of E2-induced ERK/MAPK activation in regulating some steps of the pro-apoptotic pathways is also demonstrated. These results were confirmed also in cancer cell lines expressing endogenous level of ER α or ER β . Altogether our findings indicate a new action mechanism for the E2-ER β complex pointing to the role of E2-induced rapid non-genomic signals in driving cell proliferation or apoptosis in cancer cells.

MATERIALS AND METHODS

Reagents

17 β -estradiol, 17 α -estradiol, L-glutamine, gentamicin, penicillin, RPMI-1640 and DMEM (without phenol red), charcoal-stripped fetal calf serum, and estradiol-BSA conjugate (β -estradiol 6-(*o*-carboxy-methyl)oxime:BSA, E2-BSA) were purchased from Sigma Chemical Co. (St. Louis, MO). The estrogen receptor inhibitor ICI 182,780 was obtained from Tocris (Ballwin, MO). The ERK/MAPK cascade inhibitor, U 0126, the PI3K inhibitor, Ly 294002, and the p38/MAPK inhibitor, SB 203580, were obtained from Calbiochem (San Diego, CA). Lipofectamine reagent was obtained from GIBCO-BRL Life-technology (Gaithersburg, MD). The luciferase kit was obtained from Promega (Madison, WI). GenElute plasmid maxiprep kit was obtained from Sigma Chemical Co. Bradford Protein Assay was obtained from BIO-RAD Laboratories (Hercules, CA). The polyclonal anti-phospho-AKT, anti-phospho-p38, and anti-p38 antibodies were obtained by New England Biolabs (Beverly, MA); the polyclonal anti-ER α , anti-ER β , and anti-ERK and the monoclonal anti-phospho-ERK, anti-AKT, anti-Bcl-2, anti-caspase-3, anti-poly(ADP-ribose) polymerase (PARP), and anti-actin antibodies were obtained from Santa Cruz Biotechnology (Santa Cruz, CA). CDP-Star, chemiluminescence reagent for Western blot was obtained from NEN (Boston, MA).

All the other products were from Sigma Chemical Co. Analytical or reagent grade products, without further purification, were used.

Cell culture

The ER devoid human cervix epitheloid carcinoma cell line (HeLa) (Marino et al., 2002), the ER α containing hepatoma cell line (HepG2) (Marino et al., 2002, 2003; Moon et al., 2004), and the ER β containing human colon adenocarcinoma cells (DLD1) (Fiorelli et al., 1999; Di Leo et al., 2001) were used as experimental models. Cells were routinely grown in air containing 5% CO₂ in modified, phenol red-free, DMEM (HeLa cells) or RPMI-1640 (HepG2 and DLD1 cells) media, containing 10% (v/v) charcoal-stripped fetal calf serum, L-glutamine (2 mM), gentamicin (0.1 mg/ml), and penicillin (100 U/ml). Cells were passaged every 2 days (HeLa and DLD1 cells) or every 4 days (HepG2 cells) and media changed every 2 days.

Plasmids and transfection procedures

The expression vectors for pCR3.1- β -galactosidase, human ER α (pSG5-HE0) (Marino et al., 2003), and human ER β

(pCNX2-ER β) (Ogawa et al., 1998) have been used. Furthermore an empty vector, pCMV5, was used as control (Marino et al., 2001). Plasmids were purified for transfection using a plasmid preparation kit according to manufacturer's instructions. A luciferase dose response curve showed that the maximum effect was present when 1 μ g of DNA was transfected in HeLa cells together with 1 μ g of pCR3.1- β -galactosidase to normalize transfection efficiency (~55–65%). HeLa cells were grown to ~70% confluence, then transfected using Lipofectamine Reagent according to the manufacturer's instructions. Six hours after transfection the medium was changed and 24 h thereafter cells were stimulated with 10 nM E2.

Cell viability and cell cycle

HeLa cells were grown to ~70% confluence in 6-well plates, then transfected and, after 24 h, stimulated. At different times after treatment cells were harvested with trypsin and centrifuged. Cells were stained with trypan blue solution and counted in a hemocytometer (improved Neubauer chamber) in quadruplicate. For the cell cycle analysis, 10⁶ cells were fixed with 1 ml ice-cold 70% ethanol and subsequently stained with 2 μ g/ml DAPI/PBS solution. The fluorescence of DNA was measured with a DAKO Galaxy flow cytometer equipped with HBO mercury lamp and the percentage of cells present in sub-G1, G1, S, and G2/M phases was calculated using a FloMax[©] Software.

Electrophoresis and immunoblotting

Stimulated and un-stimulated cells were lysed as described (Marino et al., 1998). When indicated 1 μ M ICI 182,780 or 10 μ M U 0126 or 10 μ M Ly 294002 or 5 μ M SB 203580 were added to the medium 15 or 30 min, respectively, before agonist stimulation. Cells were solubilized in 0.125 M Tris-HCl (pH 6.8) containing 10% SDS (w/v), 1 mM phenylmethylsulfonyl fluoride, and 5 μ g/ml leupeptin and boiled for 2 min. Proteins were quantified using the Bradford Protein Assay (Bradford, 1976). Twenty microgram solubilized proteins were resolved using SDS-PAGE at 100 V for 1 h. The proteins were then electrophoretically transferred to nitrocellulose for 45 min at 100 V at 4°C. The nitrocellulose was treated with 3% bovine serum albumin in 138 mM NaCl, 26.8 mM KCl, 25 mM Tris-HCl (pH 8.0), 0.05% Tween-20, 0.1% BSA, and then probed at 4°C overnight with either one of anti-ER α , anti-ER β , anti-phospho-ERK, anti-phospho-AKT, anti-phospho-p38, anti-caspase-3, anti-Bcl-2, or anti-PARP antibodies. The nitrocellulose was stripped by Restore Western Blot Stripping Buffer (Pierce Chemical Company, Rockford, IL) for 10 min at room temperature and then probed with either anti-ERK, anti-AKT, or anti-p38 antibodies (1 μ g/ml). Anti-actin antibody (1 μ g/ml) was used to normalize the sample loading. Antibody reaction was visualized with chemiluminescence reagent for Western blot.

RESULTS

Divergent effects of E2 in inducing cell growth in the presence of ER α or ER β

The level of exogenous ER α or ER β was assessed in HeLa cells untransfected (none) or transfected with either empty, ER α , or ER β expression vectors. The Western blot analysis (Fig. 1a) confirmed the absence of ERs in both un-transfected and empty vector-transfected HeLa cells, whereas a unique band at 67 kDa (ER α -containing HeLa cells) or at 57 kDa (ER β -containing HeLa cells) was detected. The time course of growth of HeLa cells transfected with empty plasmid or ER α or ER β expression vectors was examined in the presence of E2 and in the presence of the ER inhibitor ICI 182,780. Figure 1b shows that the growth of empty plasmid-transfected HeLa cells was not affected by E2 or ICI 182,780 suggesting that the presence of ER is necessary for the hormone effects. On the other hand, E2 was mitogen for ER α -transiently transfected HeLa cells (Fig. 1c), whereas a decrease in growth was detected after E2 stimulation in ER β -transfected HeLa cells with respect to unstimu-

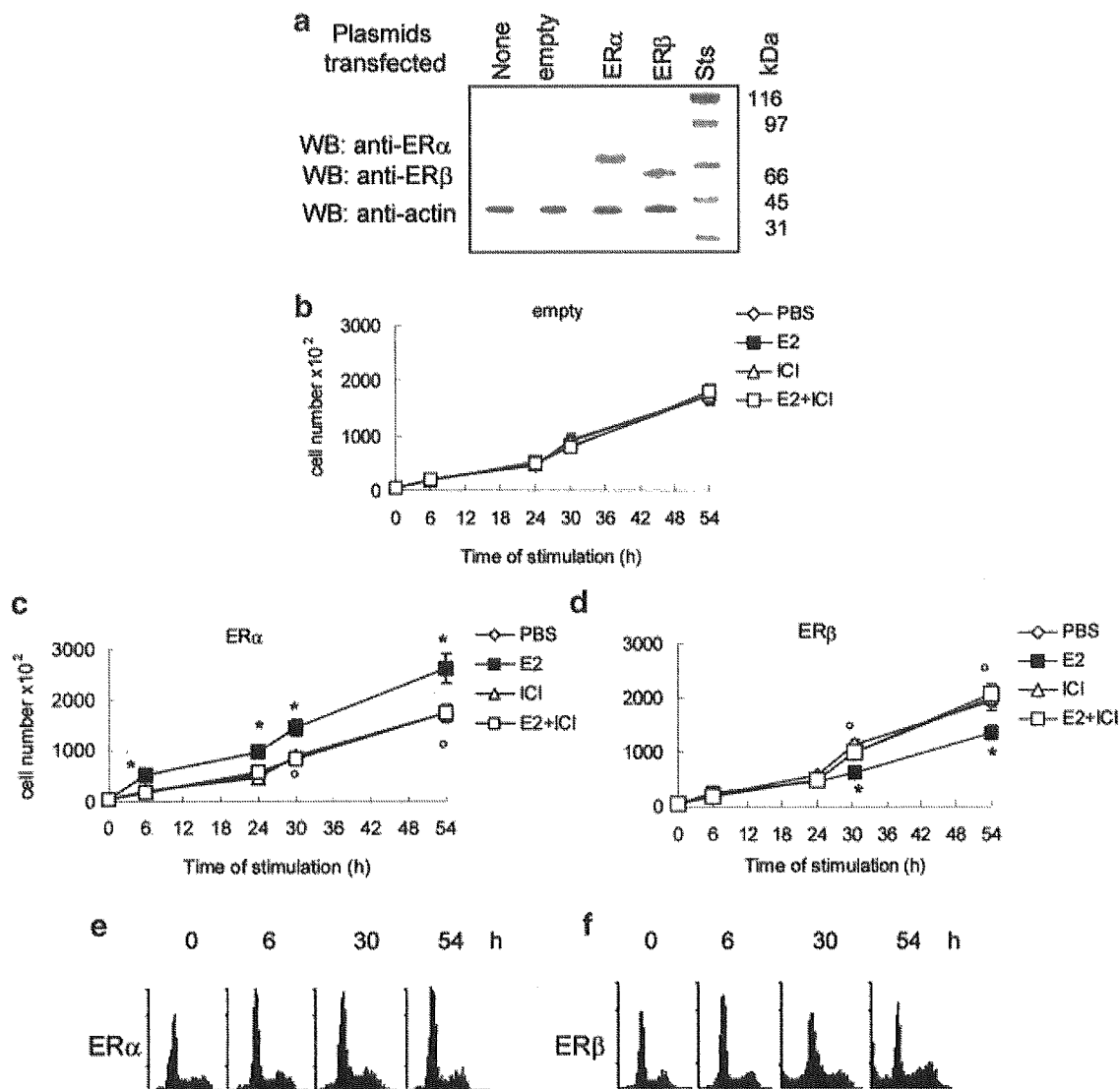


Fig. 1. Level of estrogen receptors (ERs) in transfected and un-transfected and time course of HeLa cell growth in the presence of 17 β -estradiol (E2). Western blot analysis of ER α and ER β levels were performed in un-transfected (none) or transfected HeLa cells with either empty, human ER α or human ER β expression vectors (**part a**). HeLa cells transfected with empty (**part b**) or human ER α (**part c**) or human ER β (**part d**) expression vectors were grown in DMEM in the presence of E2 (10 nM) and/or ICI 182,780 (ICI, 1 μ M) counted at the indicated times. The data are the mean values \pm SD of five indepen-

dent experiments carried out in duplicate. $P < 0.001$, calculated with Student's *t*-test, compared with respective un-stimulated values (PBS) (*) or with E2-stimulated values (\circ). Flow cytometric analysis of the HeLa cells transfected with human ER α (**part e**) or human ER β (**part f**) vectors after different time of E2-treatment compared with un-stimulated cells (0). The plots indicate cell cycle distribution present in sub-G1, G1, S, and G2/M phases, respectively. For details see the text.

lated ones (Fig. 1d). The cell pre-treatment with the ER inhibitor ICI 182,780 completely blocked the E2 effects both in ER α - and in ER β -embedded HeLa cells. Further, we analyzed, by flow cytometry, the HeLa cell cycle distribution at different time after treatment. The typical plot of plasmid transfected-HeLa cell population is illustrated in Figure 1e and f (0 h). The first peak indicates the cell number in G1 phase of the cell cycle ($50.0 \pm 5.0\%$) followed by S phase ($16.3 \pm 3.2\%$), and by the peak of G2/M phase ($19.8 \pm 2.8\%$). Increasing the time of E2-stimulation (Fig. 1e; 6, 30, and 54 h), the number of cells in G1 phase of cell cycle increased reaching $65.4 \pm 3.8\%$ 54 h after the hormone administration to HeLa cells expressing ER α . On the contrary, when HeLa cells were endowed with ER β (Fig. 1f; 6, 30, and 54 h), the number of cells in sub-G1 region increased reaching $9.5 \pm 1.0\%$ 54 h after the E2 stimulation thus suggesting the presence of DNA fragmentation.

Divergent effects of E2 in inducing an apoptotic cascade in the presence of ER α or ER β

To determine whether the reported increase of cell population in the sub-G1 phase was truthfully related to the induction of an apoptotic cascade, we analyzed the cleavage of the caspase-3 proform (32-kDa band) which results in the production of the active subunit of the protease (17-kDa band). Caspase-3 proform was expressed in HeLa cells transfected with empty or ER α or ER β expression vectors (Fig. 2a). No cleavage of caspase-3 was induced by E2 in empty or ER α -containing HeLa cells whereas E2 induced the production of the active subunit in the presence of ER β .

To confirm that the appearance in the 17-kDa band was associated with an increase in caspase-3 activity, we analyzed one of the known substrates of caspase-3, PARP. This 116-kDa, DNA repair enzyme, is cleaved by

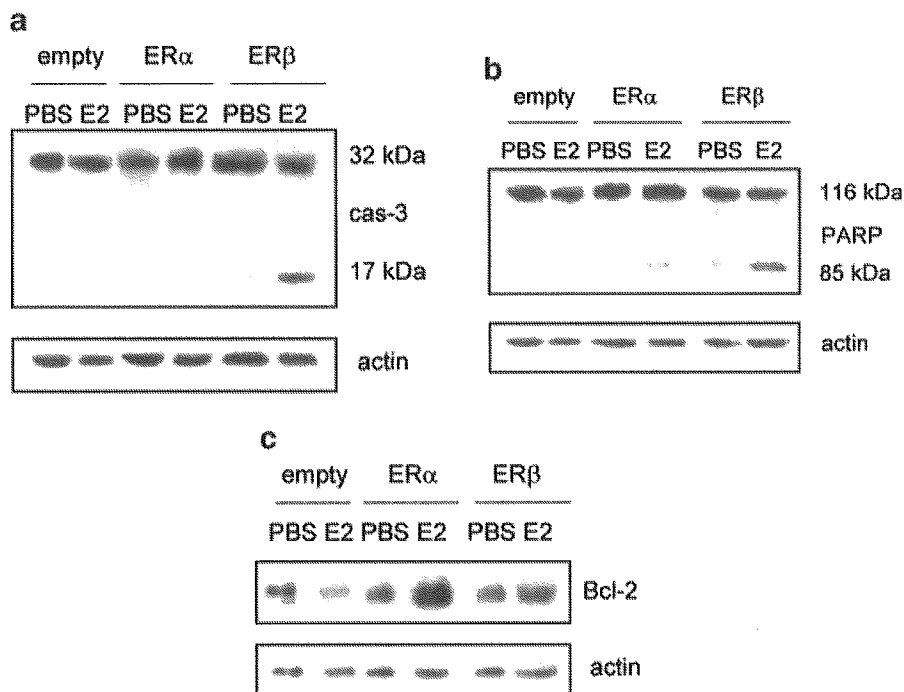


Fig. 2. Effect of E2 in the induction of pro-apoptotic proteins. Western blot analysis of caspase-3 (**part a**), PARP (**part b**) activation, and Bcl-2 (**part c**) levels were performed, as described in "Materials and Methods," on un-stimulated (PBS) and 24 h E2-treated (10 nM) HeLa cells transfected with human ER α , human ER β , or empty expression vectors. The amounts of protein levels were normalized by comparison with actin expression. Typical blot of three independent experiments. For details see the text.

the caspase-3 producing the inactive 85-kDa fragment (Fig. 2b). By Western blot analysis, treatment of empty- and ER α -containing HeLa cells with E2 did not induce any conversion of PARP in the inactive form. On the contrary, the treatment of ER β -transfected HeLa cells with E2 resulted in the conversion of PARP into the inactive 85-kDa fragment. These results were consistent with the idea that, in the presence of ER β , E2 specifically induced an apoptotic cascade involving the caspase-3 activation and a downstream substrate like PARP. This was further confirmed by the expression of Bcl-2 level, the survival factor that can block both necrotic and apoptotic cell death (Dubal et al., 1999). Only the treatment of ER α -transfected HeLa cells with E2 markedly increased the amount of Bcl-2 (Fig. 2c).

Signal transduction pathways involved in the E2-induced apoptotic cascade

We previously reported that the rapid E2-induced activation of ERK/MAPK and PI3K/AKT pathways is sufficient and necessary for E2-induced cell cycle progression (i.e., DNA synthesis and the transcription of cyclin D₁ gene) (Marino et al., 2002, 2003). Then we asked if the inhibition of these rapid signals was involved in the E2-ER β -induced apoptotic cascade.

No activation of signal transduction proteins was detected in cells transfected with empty vector and stimulated with E2 (data not shown). However, E2 increased ERK and AKT phosphorylation in HeLa cells transiently transfected with ER α (Fig. 3a). After reprobing the membranes using total ERK or AKT antibodies, to recognize the non-phosphorylated form of these proteins, the specific alteration of signaling proteins by E2 was confirmed to occur in the absence of changes in their expression levels (Fig. 3a). On the other hand, E2 failed to elicit any changes in the phosphory-

lation or expression level of ERK and AKT in cell expressing ER β (Fig. 3a). Interestingly, a similar activation was observed in cancer cell lines which express endogenous ER α (HepG2) or ER β (DLD1). In fact, E2 induced the rapid increase of ERK and AKT phosphorylation only in HepG2 cells (Fig. 3b) whereas it was ineffective in DLD1 cells (Fig. 3c). The level of endogenous ER α or ER β was assessed in HepG2 and DLD1 cells. The Western blot analysis (Fig. 3d) confirmed the presence of a unique band at 67 kDa (HepG2 cells) or at 57 kDa (DLD1 cells) corresponding to ER α or ER β , respectively.

Generally, the activation of PI3K/AKT and ERK/MAPK pathways causes cell survival in response to many mitogens and growth factors, whereas the activation of p38/MAPK has been associated with the regulation of apoptosis and differentiation processes (Ambrosino and Nebreda, 2001; Harper and LoGrasso, 2001; Talapatra and Thompson, 2001; Shimada et al., 2003; Porras et al., 2004). To verify this possibility, the effect of E2 on p38/MAPK activation was evaluated. A time course of E2-induced p38/MAPK phosphorylation in HeLa cells transfected with ER α or ER β is shown in Figure 4a. A rapid and transient increase of p38/MAPK phosphorylation was detected from 15 to 30 min after E2 stimulation in ER α -transfected HeLa cells; whereas E2 induced a rapid (15 min) and persistent (24 h) increase of p38/MAPK phosphorylation in ER β expressing HeLa cells. In the same way, E2 evoked a rapid (15 min) and transient activation of p38/MAPK in ER α -encoding HepG2 cells (Fig. 4b, upper part) and a rapid and persistent (24 h) phosphorylation of p38/MAPK in ER β -containing DLD1 cells (Fig. 4b, lower part). Note that, the E2-induced p38/MAPK activation was prevented by the pure anti-ER ICI 162,780 in either cell lines (Fig. 4b). The same inhibitor completely

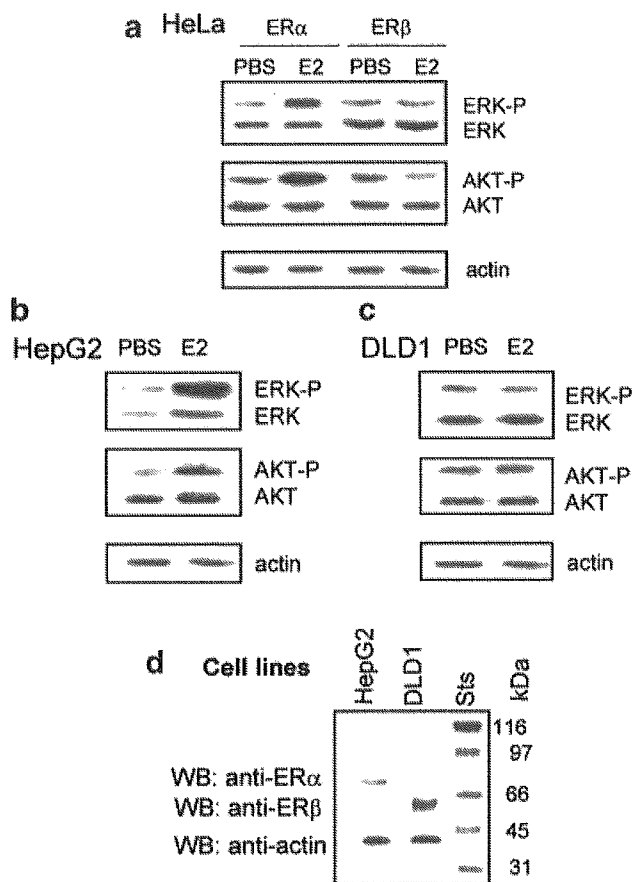


Fig. 3. Signal transduction pathways activated by E2. Western blot analysis of phosphorylated and un-phosphorylated ERK and AKT were performed, as described in "Materials and Methods," on unstimulated (PBS) and 15 min E2-treated (10 nM) HeLa cells transfected with human ER α or human ER β expression vectors (**part a**) or HepG2 cells (**part b**) or DLD1 cells (**part c**). Western blot analysis of ER α and ER β levels were performed in HepG2 cells and DLD1 cells (**part d**). The amount of protein levels were normalized by comparison with actin expression. Typical blot of three independent experiments. For details see the text.

prevented the rapid (15 min) E2-induced p38/MAPK phosphorylation also in ER-transfected HeLa cells (Fig. 4c). Furthermore, the E2 inactive stereoisomer, 17 α -estradiol, failed to induce p38/MAPK phosphorylation (Fig. 4c), whereas the E2 cell membrane impermeable, E2-BSA (Zheng et al., 1996; Marino et al., 2003), affected the p38/MAPK activation comparably to E2 (Fig. 4c). Altogether these data imply a membrane ER in the rapid and specific E2-induced activation of p38/MAPK signaling.

Cross-talk between proliferative and apoptotic signal transduction pathways and role of E2-induced p38/MAPK

The ability of E2 to induce p38/MAPK phosphorylation even in the presence of ER α was surprising and did not clarify the putative involvement of this kinase in the E2-induced apoptosis. Thus, we asked whether ERK/MAPK and PI3K/AKT cross-talk with p38/MAPK. None of the specific pathway inhibitors used (i.e., Ly 294002 and U 0126) prevented the E2-induced p38/MAPK phosphorylation in ER α -transfected HeLa cells (Fig. 5a) suggesting that the activation of this pathway was parallel and independent on ERK and AKT activation. On the contrary, the cell pre-treatment with

the same inhibitors rescued the activation of the pro-apoptotic caspase-3 (Fig. 5b) as well as completely prevented E2-induced, anti-apoptotic, Bcl-2 accumulation (Fig. 5c). The same results were obtained in HepG2 cells (Fig. 5 d, e, and f) further indicating that E2-ER α -induced ERK and AKT activation negatively modulates the apoptotic signals. To directly evaluate the role of p38 in these effects in some experiments cells were pre-treated with the specific p38/MAPK inhibitor, SB 203580 (5 μ M), before E2 stimulation. A block of p38/MAPK phosphorylation was evidenced while no effect was present on Bcl-2 levels in both cell lines considered. Note that, caspase-3 cleavage induced by E2 in the presence of U0126 was prevented by the pre-treatment of HepG2 cells with p38/MAPK inhibitor, SB 203580 (30 min) (Fig. 5g). However, the cell pretreatment with the signaling pathways inhibitors alone did not modify the p38/MAPK phosphorylation or caspase-3 and PARP cleavage.

Finally, the pre-treatment of ER β -transfected HeLa cells with the specific p38/MAPK inhibitor, SB 203580, completely prevented the formation of the caspase-3 active fragment (Fig. 6a) and the cleavage of PARP (Fig. 6b) linking the p38/MAPK activation directly to the apoptosis. As expected, E2 induced p38/MAPK-dependent caspase-3 activation in ER β -containing DLD1 cells (Fig. 6c) sustaining a pivotal role of the signaling activated by E2-ER β complex (i.e., prolonged p38/MAPK phosphorylation) in inducing the apoptotic cascade.

DISCUSSION

E2 is known to support cell survival or induce cell death/apoptosis depending on the cell context (Song et al., 2001; Song and Santen, 2003). The mechanism(s) underlying these opposite E2 effects could involve the classical/transcriptional mechanism of ER isoforms which, as ligand-dependent transcription factors, modulate the transcription of E2-induced target genes. In addition to this accepted model for the E2 action mechanism, emerging evidences indicated that rapid/non-genomic signaling molecules originating from the cell membrane are involved at least in E2-ER α -induced cell proliferation/survival (Castoria et al., 1999; Razandi et al., 1999, 2000a; Kousteni et al., 2001; Marino et al., 2001, 2002, 2003). These evidences prompted us to examine the non-genomic signaling mechanism(s) generated by the E2-ER β complex and to compare the role(s) played by these rapid signals with those generated after E2-ER α binding. Although the different functions of ER α versus ER β on cell proliferation/apoptosis balance has been suggested (Matthews and Gustafsson, 2003; Weihua et al., 2003), the contribution of signal transduction pathways generated by each isoform on these E2-induced cellular functions has not been yet clarified. Therefore, we chose the ER-devoid HeLa cells as experimental model. The transiently transfected HeLa cells allow us to discriminate the effect of each ER isoforms, without the mutual interference, in a E2-induced proliferation model (Marino et al., 2001, 2002). Furthermore, to avoid any dilemma due to the receptors over-expression, some experiments were performed in parallel in two different cancer cell lines which express endogenous ER α (HepG2) (Marino et al., 2001, 2002, 2003; Moon et al., 2004) or ER β (DLD1) (Fiorelli et al., 1999; Di Leo et al., 2001).

In these experimental conditions, E2 induced different effects on cell growth or apoptosis in dependence on ER isoform present. While the E2-ER α complex activated multiple signal transduction pathways committed to

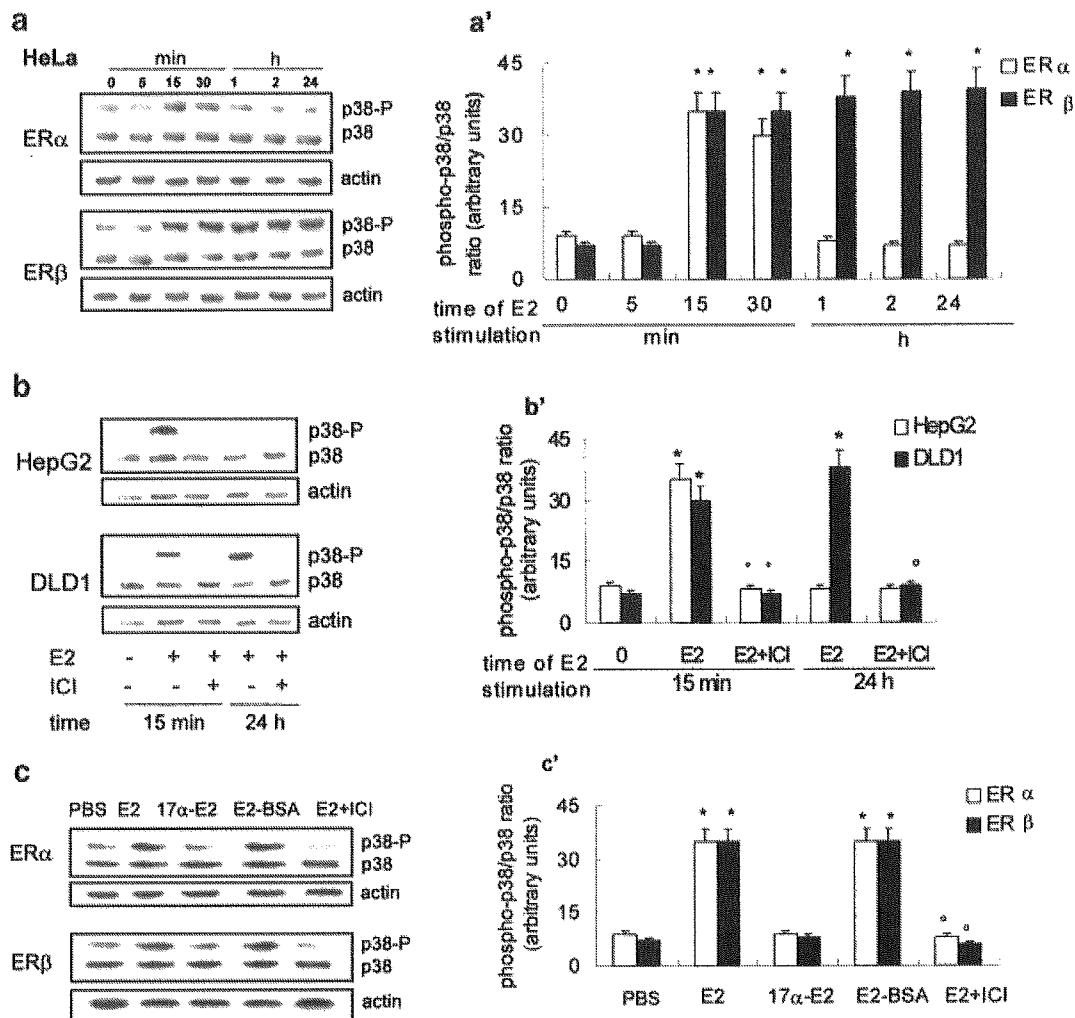


Fig. 4. Effect of E2 on p38/MAPK activation. Time course analysis of p38/MAPK phosphorylation was performed, as described in "Materials and Methods," on untreated (0, -) and E2-treated (10 nM) HeLa cells transfected with human ER α or human ER β expression vectors (parts a and a') or HepG2 or DLD1 cells (parts b and b') at the indicated times. The amount of protein levels were normalized by comparison with actin expression. Parts (a) and (b) show the typical blot of three independent experiments; parts (a') and (b') show the data obtained by densitometric analysis, mean values \pm SD. $P < 0.001$, calculated with Student's *t*-test, compared with respective un-stimulated (0, -) values (*) or with E2-stimulated values (°). For details see the text. Western blot analysis of p38/MAPK

phosphorylation was performed, as described in "Materials and Methods," in un-stimulated (PBS) or 15 min E2- (10 nM) or 17 α -estradiol- (17 α -E2; 10 nM) or 17 β -estradiol-BSA-(E2-BSA; 10 nM) treated HeLa cells transfected with human ER α or human ER β expression vectors. In some experiments cells were pretreated with ICI 182,780 (ICI) (1 μ M) before E2 stimulation. The amount of protein levels were normalized by comparison with actin expression. Part (c) shows the typical blot of three independent experiments; part (c') shows the data obtained by densitometric analysis, mean values \pm SD. $P < 0.001$, calculated with Student's *t*-test, compared with respective un-stimulated control (PBS) values (*) or with E2-stimulated values (°). For details see the text.

both cell cycle progression and apoptotic cascade prevention, the E2-ER β complex induced the rapid and persistent phosphorylation of p38/MAPK, which in turn, drove cells into the apoptotic cycle.

In the E2-stimulated ER α -containing HepG2 cells, we previously demonstrated that E2 enacted the rapid, non-genomic, and membrane starting signal transduction pathways which, in turn, worked cooperatively to achieve cell proliferation. In particular, E2-induced PKC- α was strongly related to DNA synthesis, but was not involved in cyclin D₁ transcription. On the contrary, E2-induced ERK/MAPK and PI3K/AKT pathways were strongly involved in both DNA synthesis and cyclin D₁ transcription (Marino et al., 2002, 2003). Present results clearly indicate, in well accordance with the literature (Razandi et al., 2000b; Kousteni et al., 2001), that these latter pathways have also a critical role in E2 action as a survival agent. While this work was in progress, Fernando and Wimalasena (2004) demonstrated that

the prolonged activity of AKT was required to maintain the BAD phosphorylation decreasing its pro-apoptotic effect. In addition, we demonstrate that the E2-induced rapid activation of PI3K/AKT pathway is necessary to increase the level of the anti-apoptotic protein Bcl-2 and to avoid the cleavage of caspase-3 and the induction of apoptotic cascade. Beside AKT-mediated signaling, E2 can also signal through ERK/MAPK pathway. This pathway precedes and modulates AKT phosphorylation (Marino et al., 2003). In fact, the pre-treatment of HepG2 cells with U 0126 (ERK/MAPK inhibitor) rapidly increased the levels of the tumor-suppressor, PTEN, impairing the E2-induced AKT phosphorylation (Marino et al., 2003).

Work of the last years has established that expression and function of component of death machinery are under control of signaling pathways (see Rapp et al., 2004 and literature therein). ERK/MAPK as well as PI3K/AKT cascades cooperate in cellular protection. ERK/MAPK

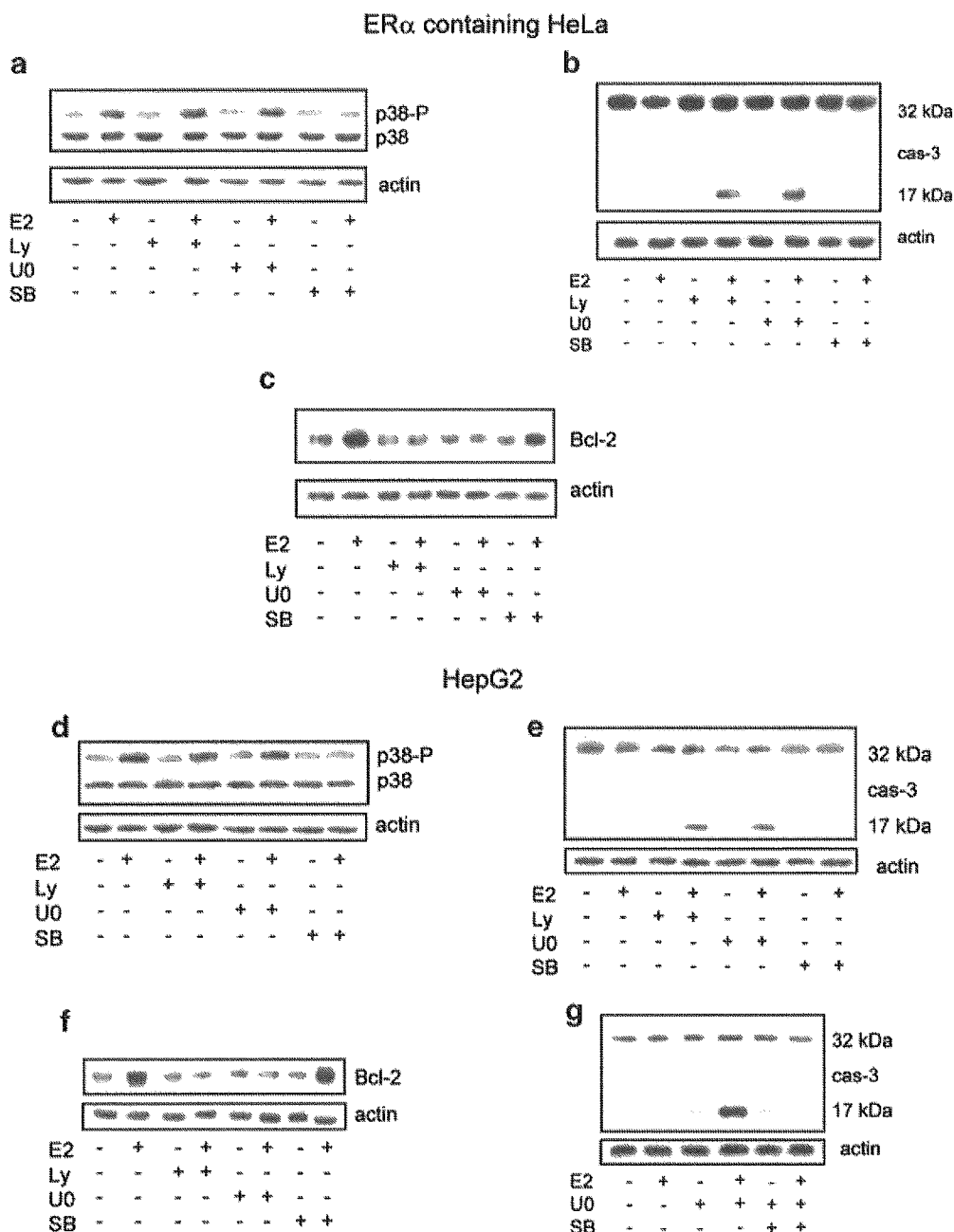


Fig. 5. Cross-talk among E2-induced ERK/MAPK, PI3K/AKT and p38/MAPK activation. Western blot analysis of p38/MAPK (parts a and d), caspase-3 (parts b, e, and g), and Bcl-2 (parts c and f) were performed, as described in "Materials and Methods," on un-stimulated (–) or E2-treated (10 nM) (15 min for p38 phosphorylation, 24 h for caspase-3 and Bcl-2 detection) HeLa cells transfected with human

ER α expression vector or HepG2 cells. When indicated 10 μ M U 0126, Ly 294002 (15 min) or 5 μ M SB 203580 (30 min) (ERK/MAPK, PI3K/AKT, and p38/MAPK pathway inhibitors, respectively) were added before E2 administration. The amount of protein levels were normalized by comparison with actin expression. Typical blot of three independent experiments. For details see the text.

control cell survival by targeting Bcl-2 to the mitochondria membranes (Tamura et al., 2004) and together with PI3K/AKT may up-regulate the expression of Bcl-2 (Rapp et al., 2004). Furthermore a direct role of PI3K/AKT in caspase-3 inhibition has been recently reported after polyamine depletion (Zhang et al., 2004). Bcl-2 overexpression, in turn, decreases intracellular Ca⁺⁺ level which can activate p38/MAPK and caspase cascades (Song et al., 2004). Our results, for the first time, show that steroid hormones may regulate this pathway. In fact, the ERK/MAPK and the PI3K/AKT pathways, rapidly activated by the E2–ER α complex, cooperatively enhance the expression of the anti-

apoptotic protein (Bcl-2), block the parallel activation of the p38/MAPK, reduce the pro-apoptotic caspase-3 activation, and promote the G1/S transition via the enhancement of cyclin D₁ expression (Marino et al., 2002, 2003; present data).

One of the main findings in this study is the different signal generated by the E2–ER β complex. There is 96% amino acid identity between the DNA-binding region (C domain) of ER α and ER β , but in the ligand-binding region (E domain) the homology is only 53% (Kuiper et al., 1998; Matthews and Gustafsson, 2003). As the E domain of ER α is sufficient to elicit non-genomic actions (Marino et al., 2002; Razandi et al., 2002; Acconcia et al.,

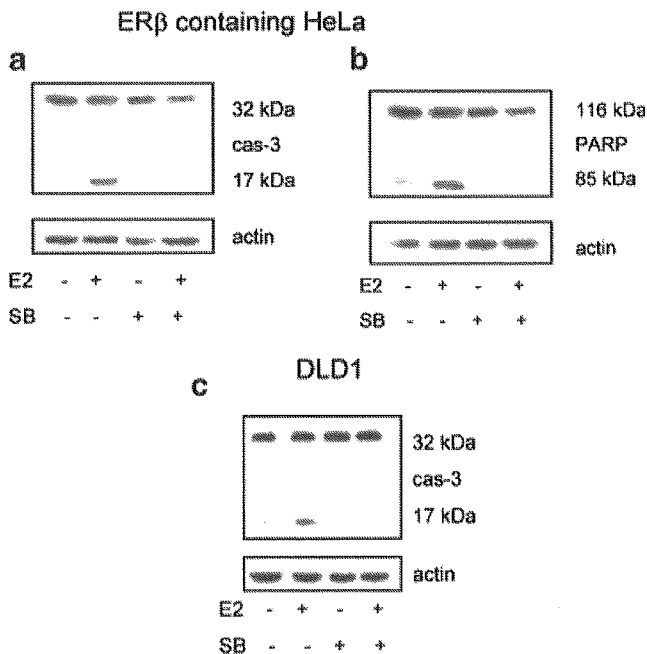


Fig. 6. Involvement of p38/MAPK in pro-apoptotic cascade activation. Western blot analysis of caspase-3 (parts a and c) and PARP (part b) activation were performed, as described in "Materials and Methods," on un-stimulated or 24 h 17 β -estradiol-treated (E2; 10 nM) HeLa cells transfected with human ER β expression vector or in DLD1 cells. When indicated 5 μ M SB 203580 (p38/MAPK cascade inhibitor) was added 30 min before E2 administration. The amount of protein levels were normalized by comparison with actin expression. Typical blot of three independent experiments. For details see the text.

2004), it is most likely that different sets of signal transduction proteins may be activated by ER α and ER β upon E2 binding. Besides these differences the two receptors display a different tissue localization and a different role in proliferation. For example, E2-ER α is a proliferative factor in the uterus, and the uterus of ER β null mice is hypersensitive to the proliferative action of E2; the co-expression of both ER isoforms is rare during the proliferative phase of mammary gland cells typical of pregnancy, whereas more than 90% of ER β -expressing mammary gland cells do not proliferate (Weihua et al., 2003); ER β is abundantly expressed in normal colonic mucosa, but declines in colon adenocarcinoma paralleling the tumor's dedifferentiation (Konstantinopoulos et al., 2003); a progressive decline of ER β expression has been found in multistage mammary carcinogenesis (Roger et al., 2001) and prostate cancer (Horvath et al., 2001). Very recently it has been reported that the induction of ER β expression reduces the growth of exponentially proliferating breast cancer cells with a parallel decrease in components of the cell cycle associated with proliferation, namely cyclin D₁, cyclin E, Cdc25A, p45^{Kip2} and an increase in the Cdk inhibitor p27^{Kip1} (Matthews and Gustafsson, 2003; Paruthiyil et al., 2004; Strom et al., 2004). Our data amplify these evidences by adding the ability of ER β isoform to rapidly induce the persistent membrane starting activation of p38/MAPK without any interference on the survival proliferative pathways, thus impairing the cell cycle components activation.

However, we were surprised to find that the E2-ER α complex increased p38/MAPK phosphorylation. Recently, Lee and Bai (2002) reported that in ER α -expressing endometrial cells, E2 activates the p38/MAPK pathway, which in turn mediates the ER α phosphoryla-

tion on threonine-311, promoting the receptor nuclear localization and interaction with specific receptor coactivators. In line with this result the E2-induced p38/MAPK phosphorylation plays a multifunctional role in cellular E2-induced effects. As discussed above, the contemporary increase of Bcl-2 levels, mediated by ERK/MAPK and PI3K/AKT pathways, may decrease the Ca⁺⁺ levels impairing the prolonged p38/MAPK activation (Song et al., 2004).

Ample evidence indicates that the p38/MAPK pathway serves an important role in stress and immune response (Han et al., 1994). Furthermore, p38/MAPK pathway has been associated with a significant slowing in cell proliferation (Han et al., 1994; Badger et al., 1996) and with the regulation of the apoptosis (Kang et al., 2003). In particular p38/MAPK can sensitize cells to apoptosis through the positive regulation of Fas/CD-95 and Bax expression which, in turn, activate caspase cascades (Porrás et al., 2004). The E2 capacity in activating p38/MAPK has been reported in a few articles and linked to the preservation of form of ER α - and ER β -containing vascular endothelial cells (Razandi et al., 2000a), or their migration and proliferation (Gerald et al., 2003), or even their apoptosis (Mori-Abe et al., 2003). Zhang and Shapiro (2000) reported the ability of E2 to induce p38/MAPK phosphorylation and cell apoptosis in a clone of ER α stably transfected HeLa cells (HeLa-ER5), unresponsive to the E2 proliferative stimuli. The reason for these disparities is not clear but could be related to the divergences in the experimental models, culture condition, E2 treatment period, proliferative capacity, or cell line variability. The E2 stimulation of two cell lines containing endogenous (DLD1) or transfected (HeLa) ER β demonstrates the ability of E2 to drive cancer cells to apoptosis via p38/MAPK-cascade.

In conclusion, besides its role as negative modulator of ER α activities, our findings indicate that ER β directs the anti-proliferative effects of E2 sustaining the tumor suppressor functions of ER β . Therefore, the expression of ERs could account for the E2-dependent modulation of cell proliferation. In particular, E2 promotes cell survival through ER α -non-genomic signaling and cell death through ER β -non-genomic signaling. Thus, the E2 opposite effects in cells co-expressing ER α and ER β could depend on the balance between the signals originated by each isoform. However, the appearance of new and different signals in the presence of either receptors can not be excluded and it is currently under active investigation in our laboratory.

ACKNOWLEDGMENTS

The generous gift of DLD1 cells from Dr. Aldo Cavallini (Biochemistry Laboratory, I.R.C.C.S.S. de Bellis, Scientific Institute for Digestive Diseases, Via della Resistenza, I-70013 Castellana Grotte, Bari, Italy) is acknowledged. The editorial assistance of Mr. Peter De Muro is also acknowledged. This work was supported by grants from FIRB 2001 and 2004 University "Roma Tre" to Maria Marino.

LITERATURE CITED

- Acconcia F, Ascenzi P, Fabozzi G, Visca P, Marino M. 2004. S-palmitoylation modulates human estrogen receptor-alpha functions. *Biochem Biophys Res Commun* 6:878-883.
- Ambrosino C, Nebreda AR. 2001. Cell cycle regulation by p38 MAP kinases. *Biol Cell* 93:47-51.
- Badger AM, Bradbeer JN, Votta B, Lee JC, Adams JL, Griswold DE. 1996. Pharmacological profile of SB 203580, a selective inhibitor of cytokine suppressive binding protein/p38 kinase, in animal models of arthritis, bone resorption, endotoxin shock and immune function. *J Pharmacol Exp Ther* 279:1453-1461.